ChemComm

ROYAL SOCIETY OF CHEMISTRY

HIGHLIGHT

View Article Online
View Journal | View Issue

Check for updates

Cite this: *Chem. Commun.*, 2023, **59**, 6109

Vacancy designed 2D materials for electrodes in energy storage devices

Rajesh Kumar, *[a] Sumanta Sahoo, *[b] Ednan Joanni,[c] Raghvendra Pandey[d] and Jae-Jin Shim *[b]

Received 21st February 2023,
Accepted 20th April 2023

DOI: 10.1039/d3cc00815k

rsc.li/chemcomm

Vacancies are ubiquitous in nature, usually playing an important role in determining how a material behaves, both physically and chemically. As a consequence, researchers have introduced oxygen, sulphur and other vacancies into bi-dimensional (2D) materials, with the aim of achieving high performance electrodes for electrochemical energy storage. In this article, we focused on the recent advances in vacancy engineering of 2D materials for energy storage applications (supercapacitors and secondary batteries). Vacancy defects can effectively modify the electronic characteristics of 2D materials, enhancing the charge-transfer processes/reactions. These atomic-scale defects can also serve as extra host sites for inserted protons or small cations, allowing easier ion diffusion during their operation as electrodes in supercapacitors and secondary batteries. From the viewpoint of materials science, this article summarises recent developments in the exploitation of vacancies (which are surface defects, for these materials), including various defect creation approaches and cutting-edge techniques for detection of vacancies. The crucial role of defects for improvement in the energy storage performance of 2D electrode materials in electrochemical devices has also been highlighted.

[a] *Department of Mechanical Engineering, Indian Institute of Technology, Kanpur 208016, Uttar Pradesh, India. E-mail: rajeshbhu1@gmail.com*
[b] *School of Chemical Engineering, Yeungnam University, 280 Daehak-ro, Gyeongsan, Gyeongbuk 38541, Republic of Korea. E-mail: sumanta95@gmail.com, jjshim@yu.ac.kr*
[c] *Center for Information Technology Renato Archer (CTI), Campinas 13069-901, Brazil*
[d] *Department of Physics, ARSD College, University of Delhi, New Delhi, 110021, India*

Rajesh Kumar

Rajesh Kumar is a Ramanujan Fellow at the Indian Institute of Technology (IIT) in Kanpur, India. His PhD in Physics was awarded by the Department of Physics at Banaras Hindu University (BHU), Varanasi, India. He had previously held positions at Korea Advanced Institute of Science & Technology (KAIST), Daejeon, and Yonsei University, Seoul, South Korea; University of Campinas (UNICAMP), Campinas, and State University of Sao Paulo (UNESP), Sao Paulo, Brazil. As a JSPS fellow, he worked at Toyohashi University of Technology (TUT), Toyohashi, Aichi, Japan. His present study focuses on innovative two-dimensional (2D) layered (organic/inorganic) materials and their applications in energy, sensors, and electromagnetic interference (EMI) shielding.

Sumanta Sahoo

Sumanta Sahoo is currently working as a Research Professor in the School of Chemical Engineering, Yeungnam University, South Korea. He received his Ph. D degree from the Indian Institute of Technology Kharagpur (IIT Kharagpur), India. His main research areas are the synthesis of graphene through chemical routes, fabrication of supercapacitor electrodes based on graphene, conducting polymer, MXene etc.

1. Introduction

Two of the most severe problems facing modern civilization are the recurring energy crises due to the dependence on quickly depleting fossil fuel reserves, and the ever increasing environmental pollution.[1–3] In an attempt to help solve both of these major issues, research in energy storage has gradually been shifted towards sustainable, "greener" technologies.[4–6] As the most promising charge storage devices, supercapacitors (SCs) and secondary batteries (like Li-ion, Na-ion, K-ion batteries, *etc.*) have been widely investigated in the recent decades.[7–14] In order to enhance the performance of these energy-related devices, the optimization of all of their components (electrodes, electrolyte and current collector) is essential. It is important to notice that although both SCs and batteries store charge through electrochemical processes, there is a distinct difference between the charge storage mechanisms in these two types of devices. While SCs (mainly electric double layer capacitors – EDLCs) store energy through the formation of doubly charged layers, the batteries rely on reversible chemical reactions. When their electrochemical performances are compared, batteries usually exhibit higher energy density, but suffer from poorer power density. However, by combining these two energy storage approaches, researchers are developing integrated devices with the potential to overcome the drawbacks of each component.[15]

Electrode materials which have demonstrated enhanced energy storage characteristics are normally those exhibiting high surface area, enhanced porosity, good conductivity, chemical stability, and a rich electrochemical activity. In this context, metal oxides (MOs)/mixed metal oxides (MMOs) have been widely investigated, mainly due to their cost-effectiveness, facile synthesis, enhanced chemical stability, and rich electrochemical activity.[16–20] Metal sulphides (MSs) and mixed metal sulphides (MMSs) have also displayed promising electrochemical performances, sometimes even better than their oxide counterparts.[21–24] For further improvement in device performance, such materials have also been integrated with other MOs, MMOs, MSs, MMSs, MXenes, conducting polymers, and carbon-based materials like graphene, carbon nanotubes (CNTs), *etc.*[21,25–33]

The electrochemical performance of any electrode for charge storage is highly dependent on its reaction kinetics. The above mentioned electrode materials sometimes demonstrate poor electrochemical performance due to sluggish kinetics. When the electrical conductivity of the electrode material is increased, reaction kinetics can be enhanced. Another approach to improve the reaction kinetics is to boost the porosity of the electrodes. By changing the intrinsic properties of the electrode materials, defect engineering also plays an important role in achieving fast reaction kinetics.[34–41] The role of crystalline defects on the electrochemical performance of electrodes has progressively been recognized though the advancement in characterization techniques, as well as in-depth theoretical studies. Several types of defects with different dimensionalities are always present in the crystalline solids, like point defects (0D), line defects (1D), planar defects (2D), and volume defects (3D). On the other hand, several approaches have been developed for

Ednan Joanni

Ednan Joanni is a materials engineer and currently a researcher at the Center for Information Technology (CTI) Renato Archer, Campinas, Brazil. He received his PhD degree from the University of Sheffield, UK in 1990. His main research interests are micro and nanofabrication, thin films, nanostructure deposition and laser processing applied to optical and electrical devices.

Raghvendra Pandey

Raghvendra Pandey is an Assistant Professor in the Department of Physics, ARSD College, University of Delhi, India. He received his PhD degree from the Indian Institute of Technology (BHU) Varanasi and later worked as INSA-JSPS fellow Postdoctoral researcher at Tokyo Institute of Technology, Japan. His research mainly focuses on the synthesis, design, development and investigation of energy materials used for fuel cells, supercapacitors, batteries, solar cells and sensors.

Jae-Jin Shim

Jae-Jin Shim is a Professor at the School of Chemical Engineering, Yeungnam University (YU), South Korea. He is now the Director of the Institute of Clean Technology and the Clean Energy Priority Research Center supported by the Ministry of Education of Korea. His current research interests are synthesis and applications of graphene (or carbon nanotube and carbon nano-onion)-based nanocomposites with metal oxides, sulfides, or phosphides for supercapacitors, catalysis, and sensors. New materials such as perovskites, MXene, LDH, and MOFs are also under investigation for energy storage, water splitting, and wastewater treatment applications.

the intentional introduction of crystalline defects. Some of the most common strategies are based on hydrothermal/solvothermal treatments, thermal treatments (by various methods), chemical reduction processes (using reducing agents), electrochemical processes, plasma treatments, ball milling, *etc.* The generation of point defects through heteroatom doping has been widely employed by researchers, modifying the electronic structure and improving the electrochemical performance of graphene.[42–45] In a similar way, inducing vacancies in metal oxides or metal sulphides has generated a positive impact on catalytic performance.[46–48] Line defects are associated with dislocation of atoms in the crystal. As an example, the epitaxial growth of ZnO on GaN thin films has been achieved through nucleation in screw dislocations.[49] On the other hand, planar defects may span whole grains, as in twin boundaries, which can act as redox active sites to boost the electrochemical performance of MOs.[50–52] Further, volume defects are mostly referred to as voids or lattice disorder. Such defects may significantly reduce the charge transfer resistance and supply additional edge sites for the improvement of electrochemical characteristics.[53,54]

In recent years, vacancy engineering has drawn considerable interest among energy researchers (Fig. 1). By inducing defects in advanced electrode materials, one can drastically manipulate their electronic state, effectively tailoring the band gap. In terms of properties, the electrical conductivity may be significantly enhanced, and the number of sites available for charge storage might be increased, improving the electrochemical performance. As an example, the introduction of oxygen vacancies significantly enhanced the photocurrent of In_2O_3 for application in water splitting.[55] Moreover, sulphur vacancies were shown to promote the photocatalytic performance of metal sulphides by inhibiting the photocorrosion and promoting charge separation.[56]

The current review article discusses the recent advances in vacancy engineering for electrochemical energy storage applications. The role of such vacancy-related defects on the electrochemical performance of 2D materials is briefly explained. Further, the main synthetic approaches to generate vacancies in electrode materials and the advanced characterization techniques for detecting vacancies are summarized. The latest research relying on the application of such vacancy-engineered electrodes to SCs and batteries is then discussed.

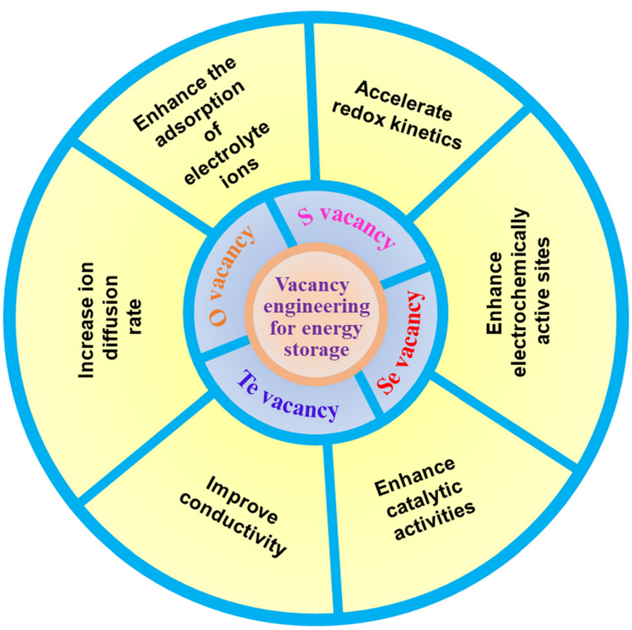

Fig. 1 Schematic diagram demonstrating the potential of vacancies defects in 2D materials for energy application.

2. Vacancy engineering in 2D materials

Vacancy engineering has significant impact on modern materials science. The structure, properties, and performance of 2D materials can be radically altered through proper controlling of vacancy concentration. Depending on the nature of charge, such vacancies can be divided into three categories: cationic, anionic, and neutral. Among these, cationic vacancies have been observed majorly in transition metal oxides/mixed metal oxides like MnO_2, Fe_2O_3, TiO_2, $ZnCo_2O_4$ *etc.*[47,57–61] However, such vacancies have been found in MXenes too.[62,63] On the other hand, anion vacancies have been frequently observed in metal oxides/mixed metal oxides, metal sulphides/mixed metal sulphides, metal selenides, tellurides *etc.*[64–68] It is important to notice that the Group-VI elements are mainly the deficient elements for generating such vacancies. The vacancies By reducing energy barriers, vacancies may significantly influence the transport-related phenomena. Neutral vacancies have been observed in carbon materials, Group-IV semiconductors *etc.*[69,70] Other monoatomic defects like C, N vacancies also play a significant role in diverse electrochemical applications like water splitting, supercapacitors, batteries, electrocatalysis, *etc.* Apart from these, multivacancies have also been introduced in metal oxides/metal hydroxides to improve the electrochemical characteristics.[71–73] When compared to monoatomic vacancies, multivacancies tend to yield better performance due to the strong synergy between different types of vacancies. Recently, dopant atoms and vacancies have been simultaneously introduced in the same material to achieve the advantages of both types of defects.[74–76] From a thermodynamic point of view, vacancies can further be categorized into two classes: equilibrium and non-equilibrium. While the non-equilibrium vacancies are related to high-energy particle irradiation, the equilibrium vacancies are more commonly present in crystals, and are found to be highly stable.

Introducing vacancies, one can trigger not only chemical changes, but also changes in the physical properties of the materials. In general, such defects induce lattice distortion, electron localization, bond disruption or bond formation. With the creation of vacancies, one can tailor the band structure, improve electronic transport, optimize reaction kinetics, increase the number of electrochemically active sites, and even enhance room-temperature magnetism. However, accurately controlling the vacancy concentration as well as adjusting their distribution are prime targets for researchers in this field.

In spite of the possible benefits of controlled defect introduction, one should always keep in mind that when the concentration of vacancies becomes too high, they can induce unit cell distortion, which causes degradation of metastable microstructures, precipitation, and an overall tendency for decreasing mechanical properties. Once again, there are good reasons for improving the control over vacancy concentration and placement.

For energy-storage applications, anionic vacancies (elements like O, S, Se, Te) have been frequently studied. The missing oxygen atoms from the metal–oxygen crystalline lattice result in the creation of oxygen vacancies. This specific defect has the ability to alter the Fermi level. Such vacancies increase the carrier concentration, improving the conductivity of the material.[77] On the other hand, S-vacancies are used to restrict the electron–hole recombination, enhancing the lifetime of electrons.[78] Such characteristics are highly desirable for photocatalytic applications. When compared to O and S vacancies, Se and Te vacancies have not been widely explored, and the influence of such vacancies on the charge storage mechanisms has not been significantly studied.

3. Development of vacancies in 2D materials

In this section, we present the prominent methods for developing vacancy defects, including microwave irradiation, ion implantation, hydrothermal and solvothermal methods, ultraviolet irradiation, plasma treatments, liquid phase exfoliation. We highlight the recently developed processing strategies and discuss in detail the formation of vacancies and some of the conditions used for their creation.

3.1. Microwave irradiation

Defective structures of 2D materials have attracted interest in the field of energy because of their large surface area, layered structure, and good physical and chemical properties.[79–88] Atomic vacancies and mesoporosity in 2D layered materials are key factors for excellent electrochemical performance. Some authors observed that unlike pristine graphene, oxygen-containing structures in graphene can stably adsorb Li atoms, enhancing their adsorption ability for CO_2.[89,90] In this study, the authors found that as the size of the O vacancies increased, the Li storage capacity was also increased.

MW irradiation can be applied to 2D layered materials, inducing atomic vacancies and surface defects, usually improving the performance of electrodes in energy-related applications. The amount of vacancy-associated defects in 2D materials can be regulated by controlling the microwave power, exposure time and by the nature of the reaction medium. WO_3 nanosheets have been synthesized using microwave-assisted hydrothermal synthesis and modified with auxiliary agents (oxalic acid, citric acid, and tartaric acid). The nanosheets exhibited O vacancies, providing high surface charge migration.[91] The creation of surface defects in graphene through microwave treatments brings benefits in various practical engineering applications. In this regard, surface defects in 3D porous graphene materials have been generated *via* microwave irradiation, with the help of Pd nanoparticles. The material has demonstrated improved performance for CO oxidation.[92] Fig. 2 displays the formation of nanoholes in porous 3D graphene using Pd nanoparticles through microwave irradiation. By stepwise increasing the power and time, the development of defects in the graphene layers increased and the Pd nanoparticles diffused into the graphene materials.

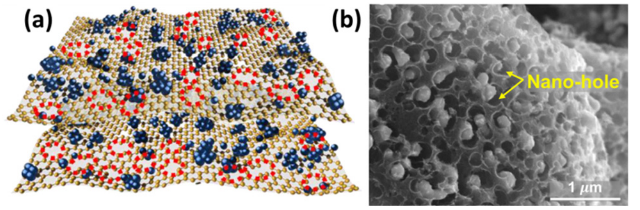

Fig. 2 (a) Schematic presentation of the microwave-assisted formation of nanoholes in graphene, and (b) SEM image of perforated graphene structures.[92] Reproduced with permission from ref. 92 Copyright 2015 American Chemical Society.

3.2. Ion implantation

Another physical method which has been used for defect creation in 2D materials is ion implantation.[93–97] Significant research has been devoted to ion implantation, which is frequently applied to modify 2D materials through the creation of vacancies, doping and intercalation. Interestingly, electron/ion bombardment of 2D layered materials creates vacancies as defects. The deviations from perfection by bombardment of materials can be used to improve some of its properties. The process has allowed researchers to tailor the local properties of the 2D materials. The ballistic ejection of carbon atoms from graphene materials by irradiation has been reported and it was responsible for the abundance of point defects.[98–100] The synthesis of engineered defects in 2D graphene materials has been extensively studied. For example, Villarreal *et al.*[101] have recently published research on defect formation in graphene materials due to the breaking of C–C bonds and development of C-substrate bonds by ultralow energy (15–40 eV) ion implantation (with He, Ne and Ar). The C–C bond defect concentration was increased with the energy and the atomic number of the implanted elements. Fig. 3 shows a schematic illustration of defects formed upon the actual removal of C atoms by ion bombardment.

3.3. Hydrothermal/solvothermal methods

The hydrothermal/solvothermal methods allow researchers to study the creation of atomic vacancies during the synthesis of 2D materials. As an example, MnO_2 ultra-thin nanosheets with high specific surface area have been synthesized by a hydrothermal method. The material contained abundant O vacancies which enhanced its catalytic oxidation performance.[102]

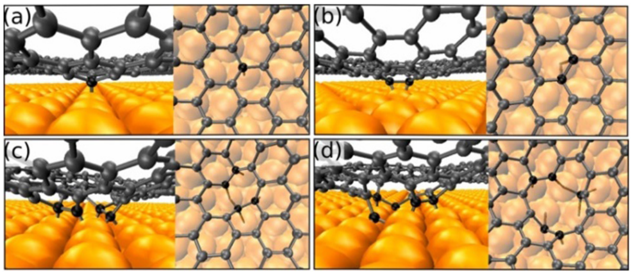

Fig. 3 Snapshots of simulations for (a) one bond defect (b) two bond defects (c) four bond defects and (d) five bond defects after a single ionic impact.[101] Reproduced with permission from ref. 101 Copyright 2023 Elsevier.

The surface atoms simply break away from the crystalline lattice, leaving vacancies in the material. In another work, layered BiOCl nanosheets with huge O vacancies have been produced *via* a solvothermal method using $Bi(NO_3)_3{\cdot}5H_2O$ and glycerol as solvent at 160 °C. In addition to anionic vacancies, cationic vacancies in 2D materials may also have a significant impact over the electronic structure, and ultimately the properties. Defective one-unit-cell $ZnIn_2S_4$ atomic layers have been synthesized *via* a hydrothermal treatment using $Zn(NO_3)_2$, $In(NO_3)_3$, L-cysteine and DI water at 200 °C.[103] The Zn vacancy concentration was tuned by changing the hydrothermal temperature. A one-unit-cell $ZnIn_2S_4$ layer with tunable defect concentration (Zn vacancies) is shown in Fig. 4. Sulphur vacancies in single-unit-cell $CuIn_5S_8$ layers were created *via* a solvothermal-assisted heating process.[104] Initially, $InCl_3{\cdot}4H_2O$, $Cu(CH_3COO)_2{\cdot}H_2O$ and ethylene glycol (as solvent) were solvothermally treated at 180 °C. In sequence, the mixture was rapidly heated (450 °C, 2 min) in 5% Ar atmosphere. Based on the above examples, one can notice that hydrothermal/solvothermal methods can be applied for generating both kinds of vacancies (anion or cation) by simply changing the precursor materials and/or the solvent.

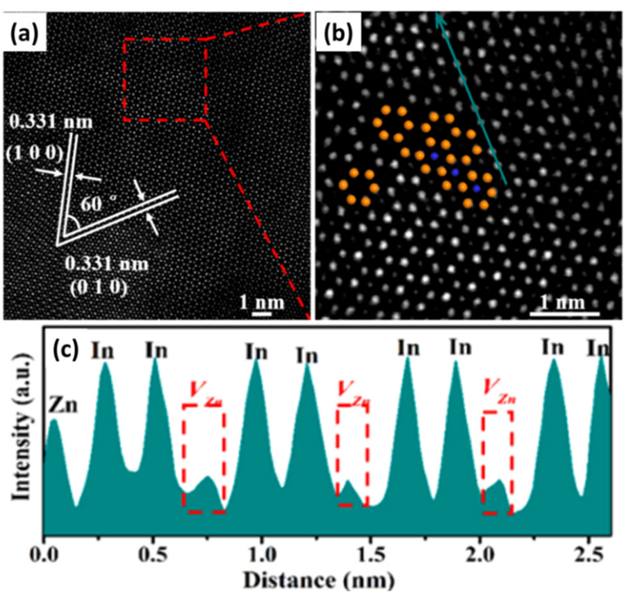

Fig. 4 Zn vacancy-rich one-unit-cell $ZnIn_2S_4$ layers (a and b) HAADF-STEM images and (c) intensity profile corresponding to the dark cyan arrow in (b), demonstrating Zn vacancies in the atomic layer.[103] Reproduced with permission from ref. 103 Copyright 2017 American Chemical Society.

3.4. Ultraviolet irradiation

Ultraviolet irradiation has also been applied to form O vacancies in layered materials.[105] Several researchers have observed that UV light irradiation produce O vacancies in BiOCl.[106–108] Due to low bond energy as well as long bond length between Bi and O in BiOCl, the Bi–O bond is easily broken by high-powered UV irradiation, leaving O vacancies. *In situ* generation of O vacancies in BiOCl nanosheets under UV light has been reported using $Bi(NO_3){\cdot}5H_2O$, KCl and NaOH.[107] In this study, the authors observed that in the (001) surface of $BiOClO_2$ is preferentially reduced to $^{\bullet}O_2^{-}$ by 1-electron transfer, however the (010) surface favours the formation of O_2^{2-} *via* 2-electron transfer. The process was governed by the different surface atomic structure and also by *in situ* produced O vacancy characteristics of (001) and (010) surface under UV light irradiation.[107] In another study, BiOCl with O vacancies was prepared using $BiCl_3$, triethanolamine, *p*-benzoquinone, nitroblue tetrazolium, C_2H_5OH and NaOH. The mixture was irradiated with UV light under Ar blowing.[108]

3.5. High temperature treatment under gas atmosphere

Thermal treatments carried out under a controlled gas atmosphere have been widely used for developing O vacancies in 2D materials. WO_2–carbon mesoporous materials were prepared *via* calcination of inorganic/organic WO_3–ethylenediamine hybrid precursors (700 °C, Ar gas flow). The products contained a large amount of O vacancies, exhibiting high performance in HER reaction.[109] NiSe/FeSe nanocubes with Se vacancies wrapped by N-doped porous graphene have been synthesized *via in situ* carbonization and selenization processes for improved Na/K storage. The material revealed fast ion transport kinetics and enhanced conductivity.[110] Nanosheets of g-C_3N_4 with variable N vacancies, processed in hydrogen atmosphere at different temperatures (475 to 550 °C) have been reported by Tu *et al.*[111] The authors observed that yields of g-C_3N_4 nanosheet materials with N vacancies was 80%, 56%, 42%, and 33%, when heated at 475, 500, 525, and 550 °C, respectively. The transmission electron microscopy revealed a thin, porous, and flexible sheet-like morphology (Fig. 5a). A schematic drawing of a tunable N vacancy in a g-C_3N_4 nanosheet is displayed in Fig. 5b.

3.6. Plasma treatment

Plasma treatment at low temperature develops surface vacancies in 2D materials, and is generally applied in low pressure treatments. Plasma treatments are categorized into high-temperature and low-temperature. High-temperature plasma treatments are usually found in nuclear applications; however low-temperature plasmas (including thermal and cold plasmas) is applied for synthesis and modification of materials structures.[112,113] In cold plasma, the temperature achieved by

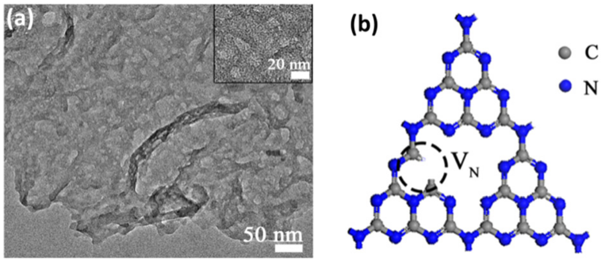

Fig. 5 (a) TEM image of g-C_3N_4 material prepared at 525 °C and (b) schematic of g-C_3N_4 with nitrogen vacancies.[111] Reproduced with permission from ref. 111 Copyright 2017 American Chemical Society.

electrons is nearly 10^4–10^5 K (1–10 eV), however the gas as a whole remains at room temperature. Cold plasma treatments applied to 2D materials generates surface defects within a very short time, when compared to other synthesis methods.[113] Using dielectric barrier discharge plasma treatments, O vacancies have been introduced into ultrathin pristine Bi_2WO_6 nanosheets in Ar atmosphere.[114] A 15 min treatment to Bi_2WO_6 ultrathin nanosheets by dielectric barrier discharge was enough to generate a high concentration of O vacancies when compared to pristine Bi_2WO_6 nanosheets.

Ar plasma treatment has been widely used for the creation of vacancy defects in nanosheets.[115] A mild Ar plasma treatment was applied to develop S vacancies in MoS_2 monolayer.[116] By tuning the Ar plasma exposure time on MoS_2 materials, the concentration of S vacancies was controlled. Ar plasma was developed with the help of 4 W RF power in a 15.2 cm diameter vacuum chamber at 1 bar pressure. In another research work, a high amount of surface defects have been created into g-C_3N_4 by Ar plasma treatment.[114] Initially, g-C_3N_4 materials were placed into a quartz tube furnace and Ar-plasma treatment was carried out in a plasma-enhanced CVD furnace with optimized conditions (power: 200 W, Ar flow rate: 50 mL s^{-1}, pressure: 40 Pa). The complete process for the formation of defects in g-C_3N_4 using Ar plasma is displayed in Fig. 6.[114]

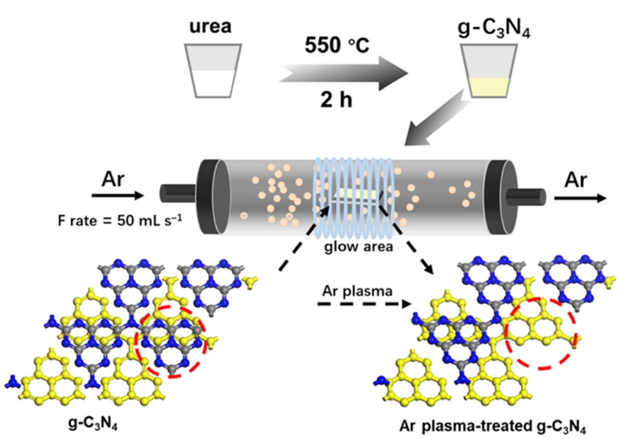

Fig. 6 Schematic representation for plasma treatments of g-C_3N_4 containing a high concentration of surface defects.[114] Reproduced with permission from ref. 114 Copyright 2020 Elsevier.

3.7. Liquid phase exfoliation

Liquid-phase assisted exfoliation process is an effective approach to produce 2D materials rich in vacancies.[117] Using liquid phase exfoliation, O vacancies have been developed in monolayer BiOBr nanosheets with the help of formamide.[118] In this process, to create the O vacancies, monolayer BiOBr nanosheets were added to a formamide solution and then stirred (260 rpm, 6 h) along with ultrasonication. Due to the mechanical stresses by stirring/ultrasonic treatment, BiOBr lamellas experienced lateral sliding, and finally the monolayered BiOBr nanosheets with O vacancies were obtained. The schematic representation of this process is shown in Fig. 7.[118] Also, BiOBr ultrathin nanosheets containing Bi vacancies have been synthesized *via* centrifugation process using liquid phase exfoliation in the presence of ionic liquids.[119] In this process, BiOBr was centrifuged at 1000 rpm and 12 000 rpm, and after that washed with H_2O and C_2H_5OH to achieve the Bi deficient BiOBr ultrathin nanosheets.

3.8. Other methods

Other techniques have also been applied to 2D materials in order to generate vacancy defects. A template-assisted strategy is one of these approaches. In this way, a soft template approach has been suggested for preparation of mesoporous MoO_{3-x} nanocrystalline walls containing O vacancies. The defects played a key role in the electrochemical performance.[120] The CVD technique has also been suggested for defect formation in 2D materials. Oxygen vacancy-rich porous MnO/graphene arrays were grown on flexible nanoporous Cu–Mn substrates through CVD and hydrogen etching.[121] The electrode material exhibited structural stability, fast charge-transfer, effective lithium-ion diffusion, and good storage performance. Ball-milling has been reported as another method to change the original structure, creating vacancies in 2D materials. Ball-milled

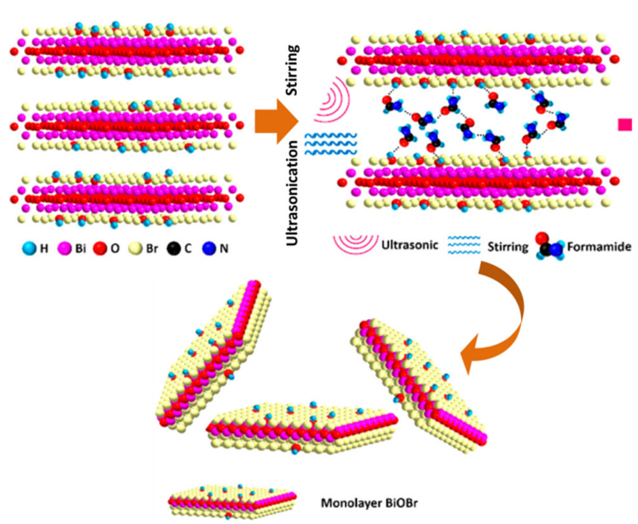

Fig. 7 Schematic representation for the formation of O vacancies in monolayered BiOBr nanosheets *via* liquid exfoliation by stirring and ultrasonication.[118] Reproduced with permission from ref. 118 Copyright 2017 American Chemical Society.

graphite powder has been shown to contain a large number of edge and surface defects.[122] Also, two types of defects (Bi and O vacancies) were found in $BiPO_4$ materials by ball-milling.[123] Pristine $BiPO_4$ was mixed in C_2H_5OH and ball-milled at 300 rpm for 2 h. After drying in air, the powder was calcined at 200–600 °C for 4 h.

4. Tools for detection of vacancies

Although many researchers have reported the presence of vacancies and surface defects in 2D materials using various characterization methods, however still difficult to accurately quantify the concentration of vacancies.[124] In this section we provide a concise summary of the cutting-edge characterization techniques toward defects analysis.

4.1. Electron paramagnetic resonance

Electron paramagnetic resonance (EPR) spectroscopy has been applied as a useful technique for studying the magnetic moment from unpaired electrons due to the transitions between energy states.[125] EPR spectra can be interpreted for a small subset of paramagnetic species, making it a useful tool for studying complex materials. Single-electron-trapped vacancy defects in materials have been detected using EPR spectroscopy.[55] The types of defects and their relative concentrations may be determined by varying g values and signal strengths. The EPR technique has been used to extensively probe the structural defects of graphene oxide.[126] Due to the extended spin relaxation periods indicated by the small line width of the EPR component, it is probable that the defect-associated spins are oxygen-centred radical species resulting from the redox response of the oxygenated groups.[127,128] An EPR signal is produced at g = 2.004 if a single electron is trapped in a vacancy.[129–132] A BiOCl-based structured material produced a signal at g = 2.001 in the EPR spectra, providing conclusive evidence for the presence of O-vacancies.[133]

4.2. X-ray photoelectron spectroscopy

X-ray photoelectron spectroscopy (XPS) is a very sensitive spectroscopic method for determining the atomic composition and chemical state of elements on surfaces.[134,135] The XPS is able to reflect surface information of materials since its testing depth is so shallow (a few nanometers). As a result of the atomic thickness of 2D materials, the measured XPS response, closely matches the actual state of the material as a whole. Changes in bonding energies, or the formation of new bonds as a result of flaws induced in the 2D material network can be detected in the spectrum as a peak shift or as a new peak. Based on the relative element concentrations, bonding energy values, and peak strength ratios, a comprehensive defect statistics for a 2D material might be attained. Further changes in the XPS spectra of the atoms surrounding the vacancy element provide additional evidence of vacancy creation. XPS analysis has been performed to assess the presence of S vacancies in 2D $ZnIn_2S_4$ nanosheets.[136] Information about the presence of oxygen vacancies in 2D MnO_2 nanosheets has also been collected using XPS.[102]

4.3. X-ray absorption fine structure spectroscopy

X-ray absorption fine structure (XAFS) spectroscopy allows for a more comprehensive analyses of defects, when compared to XPS.[137–140] The XAFS technique is applied to 2D materials using synchrotron radiation in order to ascertain the local atomic and electronic structures, providing exact information, down to very minor alterations. XAFS may be used to gather knowledge about oxidation states, types of bonding, bonding lengths, bonding angles, and atomic coordination numbers. This strongly implies that XAFS is well suited to studying defects present in 2D materials.

4.4. Positron annihilation spectroscopy

Positron annihilation spectroscopy (PAS) provides a non-destructive approach for the characterization of a wide range of defects (from single vacancies up to mesopores). In order to differentiate between the inherent defects in 2D materials, PAS has been shown to be an effective method for vacancy-type defects investigation.[141,142] Thermalization and annihilation by electrons upon the positron insertion in the material results in the emission of photons that provide information on positron lifetimes. The creation of vacancies can be detected using PAS, and the nature of those vacancies may also be identified. When vacancies are created in 2D materials, a certain range of lifetimes becomes more dominant. As a result, a vacancy may be identified by observing a shift in the relative intensity of a single component, and the kind of vacancy can be determined by counting the number of lifetime fitting parameters.[71,143–145] Positrons tend to concentrate in areas with low electron density, like vacancy-type defects, vacancy clusters, and microvoids, in contrast to the rest of the material.[146] PAS has been used to characterize the negatively charged vacancy defects present in 2D sheets.[147] The dissimilar positron lifetimes allow for the differentiation of vacancy types and the determination of relative concentrations. For example, the $V_{Bi}'''V_{O}^{\bullet\bullet}V_{Bi}'''$ vacancy (∼325 ps) connections have been observed as defects in BiOCl nanosheets, whereas isolated Bi vacancies (∼250 ps) are mostly in BiOCl nanoplates, based on the different positron annihilation lifetimes for these two types of defects (Fig. 8).[147]

4.5. Raman spectroscopy

The basic structural characteristics of 2D materials are often investigated using Raman spectroscopy.[148–151] Raman spectroscopy measures vibrational level changes from molecules *via* the Raman shift.[152] It is the vibration modes of the various chemical bonds and ground states that define the magnitude of the energy gap between them. The structural properties of crystals may be investigated by using the Raman shift, which is connected to lattice vibrational modes. Vibrational modes may be tuned by flaws in materials, notably in ultrathin 2D crystals, leading to a shift, or to the appearance of new peaks in the Raman spectrum. Using Raman spectra, various 2D

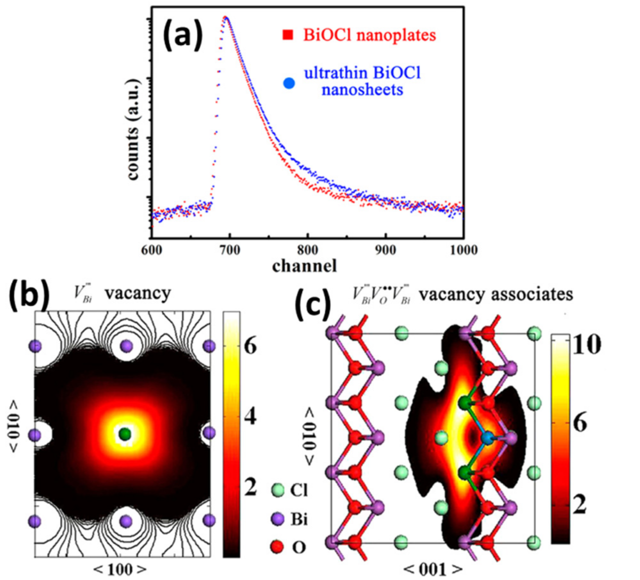

Fig. 8 PAS of BiOCl nanosheets and BiOCl nanoplates. (a) Positron lifetime spectrum. Schematic view for trapped positrons of (b) V_{Bi}''' defect and (c) $V_{Bi}'''VO^{\bullet\bullet}V_{Bi}'''$ vacancy.[147] Reproduced with permission from ref. 147 Copyright 2013 American Chemical Society.

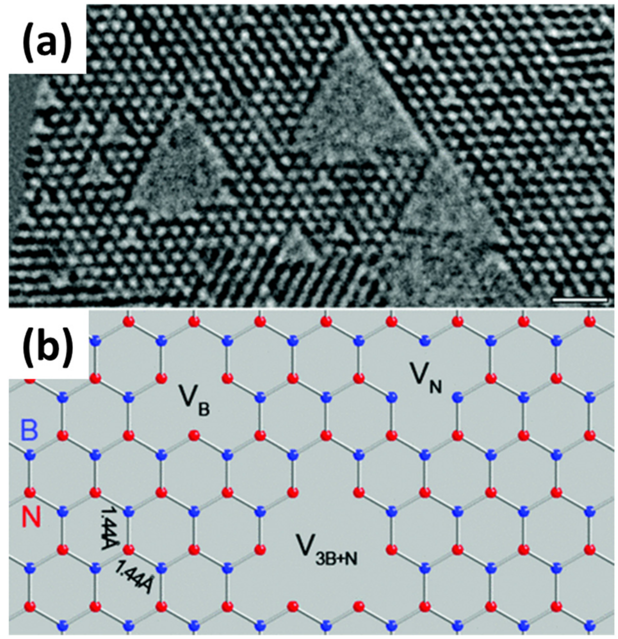

Fig. 9 (a) HR-TEM image of lattice defects in h-BN (Scale bar = 1 nm). (b) Model for the atomic defects in h-BN.[156] Reproduced with permission from ref. 156 Copyright 2009 American Chemical Society.

materials have been characterized, regarding the layer thickness and phases present in the material.[153] A single Se vacancy is responsible for the emergence of a Raman peak at 250 cm^{-1} in $MoSe_2$, as calculated by density functional theory (DFT), and this mode is an A_{1g}-like localized mode, as validated by polarized Raman scattering experiments.[154]

4.6. High-resolution microscopy

Rapid advances in electron microscopy technology have made it possible to directly image the atomic structure of 2D materials, complementing the spectroscopic studies.[103,155] Defect types may be detected and even counted by comparing the brightness of individual atoms. The atomic arrangement in the crystal, and spot deficiencies can also be studied by high-resolution electron microscopy. High-resolution transmission electron microscopy (HR-TEM) is often utilized in the characterization of vacancies. In the HR-TEM micrographs, induced defects in single layer h-BN often take the appearance of triangle-shaped holes (or vacancies) of varying sizes, but maintaining the same orientation.[156] Since boron and nitrogen atoms could not be differentiated, it was not possible to determine the precise atomic structure of these defects (Fig. 9a). In particular, vacancy of B and vacancy of N should be oriented in the opposite direction, whereas a vacancy of B and a vacancy of B + N defects surrounded by two-coordinated N atoms should both display the same orientation (Fig. 9b).

5. Energy related applications

Vacancy engineering plays a significant role in energy storage applications, and this becomes evident from the rapidly increasing number of scientific publications in recent years. The two main reasons for introducing defects in charge storage materials are the improvement in the intrinsic conductivity, as well as the increase in the number of lattice sites for pseudocapacitive charge storage. In recent years, advanced materials like metal oxides/mixed metal oxides, LDHs, MXenes, perovskites *etc.* have been treated for creating defects, in order to improve the electrochemical performance of the materials for different energy-related applications.

The role of vacancy is different for supercapacitor and batteries. For supercapacitors, the vacancies act as the active sites as well as reprieve the electrochemical strains during cycling test. Moreover, the formation of vacancies also resulted in the expansion of interlayer distance to enhance the ion intercalation pseudocapacitance. On the other hand, in case of batteries, the formation of vacancies prevent the uninvited phase transformation and reduce the energy barrier to accelerate the diffusion of metal cations.

5.1. Supercapacitors

Vacancy engineering has a positive impact on the active materials for electrodes in energy-related applications, like supercapacitors. The creation of vacancies generates many physical and chemical changes, such as lattice distortion, shifting of the band gap, electronic rearrangement, change in ionic mobility, *etc.*[157] Such significant changes can be used to improve charge kinetics, ultimately enhancing the charge storage ability of the devices.

5.1.1. Oxygen vacancies. Metal oxides are one of the most widely investigated components of supercapacitor electrodes. The charge storage characteristics of MOs has been improved by their pseudocpacitive nature. Development of studies in this research field led to the formation of binary, ternary, as well as quaternary mixed MOs. The electronic properties of such MOs can be tailored by creating oxygen-vacancies. The improvement in conductivity through oxygen vacancies has been found to be an efficient strategy for improving the capacitive nature of the MO-based electrodes.[22,158–162] A recent study has demonstrated that the introduction of Pd nanoparticles into Co_3O_4 leads to the formation of oxygen vacancies.[163] However, the study showed that the increase in the number of oxygen vacancies results in the decrease of the crystallinity of the MO. However, low crystallinity has a positive impact on the capacitive performance of MO-based SC electrodes. A similar phenomenon has also been observed for other metal oxides.[164,165] Notably, the introduction of vacancy resulted in a two-fold increment in the capacitance of Co_3O_4.

Apart from the capacitance, oxygen vacancies can improve the rate capability as well as the cycling stability of supercapacitors based on MOs. For example, oxygen-vacancy rich Co_3O_4/graphene composites displayed better rate capability (capacitance retention of 85.8% from 1 to 10 A g^{-1} current density) and cycling stability (capacitance retention of 99.3% over 20 000 cycles) than pure Co_3O_4.[166] The observed enhancement in the electrochemical performance was further supported by the results of theoretical DFT studies. The higher density of states of the MO in the presence of oxygen vacancies clearly improved charge-transfer. In fact, such oxygen vacancies acted as electron reservoirs for the electrochemical processes. Researchers undertaking similar studies have also observed drastic improvements in the electrochemical performance of Co_3O_4 with high oxygen vacancy content.[98,167] Such improvement has also been reported for vacancy-engineered lithiated Co_3O_4.[168] The controlled lithiation process was conducted through solvothermal processing (Fig. 10a). The induction of vacancies can develop a new electronic state, which has been confirmed by the DFT calculations (Fig. 10b). Moreover, the oxygen-vacancies drastically enhanced the charge carrier density (Fig. 10c). From the optimization of structural models, it has also been confirmed that the lithiated Co_3O_4 displayed higher adsorption ability as well as better stability for the electrolyte ions (OH^-) during electrochemical testing (Fig. 10d). Such defect-induced strategies were further implemented to other MOs, like MnO_2,[153,169,170] CeO_2,[171] Bi_2O_3,[172,173] MoO_{3-x},[174] WO_3,[175] Fe_2O_3.[176,177] Besides the common KOH electrolyte, such vacancy engineering has been found to be beneficial for devices based on other aqueous electrolytes, like Na_2SO_4.[66,169] The ion diffusion in MnO_2 has been altered in the presence of oxygen vacancies, as expected. The defects reduced the energy barrier for the diffusion of solvated Na^+ ions during the charge storage process, improving the pseudocapacitance. The enhanced cycling stability of such defective MnO_2 can be attributed to the easier movement of Na^+ ions among the layers of MnO_2. Additionally, the increase in surface area through the creation of oxygen vacancies also helped to improve the electrochemical characteristics. The researchers have also concluded that the larger amounts of oxygen vacancies generated a larger number of delocalized electrons, also helping to enhance the conductivity of the MOs.[153]

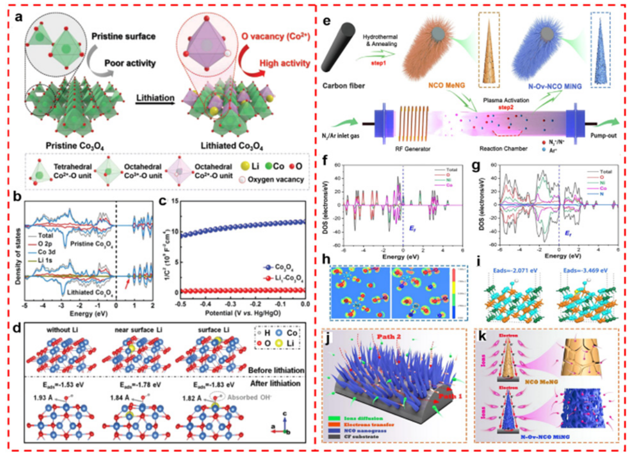

Fig. 10 (a) Schematics for the synthetic approach of lithiation-induced vacancy engineering of Co_3O_4; (b) the density of state profiles and (c) Mott–Schottky profiles for the bare Co_3O_4 and the lithiated Co_3O_4; (d) the structure of Co_3O_4 before and after the lithiation process.[168] (e) Schematics for the synthesis of N-doped and oxygen vacancy-induced $NiCo_2O_4$, grown on carbon fibres; density of state profiles for (f) $NiCo_2O_4$ and (g) N-doped and oxygen vacancy-induced $NiCo_2O_4$; (h) charge-density differences and (i) OH^- adsorption energy of $NiCo_2O_4$ and N-doped and oxygen vacancy-induced $NiCo_2O_4$. (j) Charge storage mechanism indicating the pathways for electron transfer and ion diffusion. (k) Detailed schematics for the charge storage mechanisms in MMO and defective MMO.[75] Reproduced with permission from ref. 75, 168 Copyright 2020 Wiley and 2022 Elsevier.

Oxygen vacancy engineering also plays a significant role in the improvement of electrochemical performance for mixed metal oxides. Among different MMOs, $NiCo_2O_4$ has been widely used in supercapacitor electrodes due to its enhanced conductivity, as well as its rich redox chemistry. Along with heteroatom doping, the introduction of oxygen vacancies has a great impact on the electrochemical performance of $NiCo_2O_4$. For example, the N-doped and high oxygen vacancy-induced $NiCo_2O_4$ demonstrated a high capacitance of 2986.25 F g^{-1} at the current density of 1 mA cm^{-2}, and enhanced cycling stability, with a 96.5% capacitance retention after 12 000 charge/discharge cycles.[75] The authors adopted a plasma enhanced CVD approach for introducing oxygen vacancies and N doping in $NiCo_2O_4$ grown on carbon nanofibers (CNFs) (Fig. 10e). The presence of oxygen vacancies was confirmed from a lowering of the band gap, as seen from the density of states (DOS) profiles (Fig. 10f and g). Moreover, the vacancy-induced MMO displayed higher charge density than the pristine MMO, promoting the electrical conductivity (Fig. 10h). Furthermore, calculations of OH^- adsorption energy demonstrated a rich redox kinetics for $NiCo_2O_4$ in the presence of vacancies (Fig. 10i). A higher OH^- adsorption energy for the defective MMO indicates its ability to capture a higher number of electrolyte ions. The schematics in Fig. 10j and k demonstrates the structural benefits of vacancy-induced MMO for faster electron and electrolyte ion transport.

It is important to notice that, similarly to what happens in MOs, the formation of oxygen vacancies reduces the crystallinity of MMOs too.[178] However, such decline in crystallinity does not deteriorate the capacitive properties of MMOs. Notably, the morphology of MMOs remains intact upon vacancy creation. For example, the introduction of oxygen vacancies in $NiCo_2O_4$ nanowires and nanosheets improved their capacitive performance, despite worsening their crystallinity.[179] Apart from conventional supercapacitors, such defect-induced strategy have also been employed to improve the electrochemical performance of $NiCo_2O_4$-based aqueous Zn-ion supercapacitors.[180,181]

Among the different synthetic approaches for creating oxygen vacancies, the post thermal annealing process is the most common one. By varying the annealing atmosphere, one can control the percentage of oxygen vacancies. Feng *et al.* observed an increase in oxygen vacancies for $CuCo_2O_4$ coated on Ni foam (from 59.4 to 72.9%) by changing the annealing atmosphere from pure O_2 to a mixture of N_2 and O_2.[182] Like other MOs and MMOs, the crystallinity was decreased by increasing the concentration of oxygen vacancies. However, the improvement in current response can be seen from the comparative CV profiles of the vacancy-induced MMOs. In another work, the simultaneous introduction of F dopant and oxygen vacancies improved the capacitive performance of Co_2MnO_4 coated on CF.[183] The combined heteroatom doping and vacancy creation reduced the band gap of Co_2MnO_4 from 0.35 to 0.13 eV, which improved the electrical conductivity. As a result, the defective MMO displayed specific capacity of 269 mA h g^{-1} and cycling stability of 93.2% after 5000 cycles. Unlike other MMOs, the introduction of oxygen vacancies could not decrease the crystallinity of $ZnCo_2O_4$.[184] The sheet-like morphology was also well-preserved after the the vacancy generation. Owing to the rich redox activity, such defective MMO displayed an enhanced cycling stability of 95.5%, which was found to be higher than its pristine MMO counterpart (91.6%).

5.1.2. Sulphur vacancies. Regarding its pseudocapacitive performance, metal sulphides (MSs) are found to be superior than MOs, because of their enhanced conductivity. In such MSs the sulphur vacancies played a vital role in enhancing the electrochemical performance. In this context, a recent study demonstrated the superior electrochemical performance of metal–organic framework (MOF)-derived S-vacancy induced NiS/C composite.[185] Despite the induced lattice distortion in the composite, the S-vacancies enhanced the electrochemically active sites by increasing the amount of cations having low oxidation states. As a result, the defective MS/C composite exhibited better electrochemical performance than MOF-derived NiO/C. Interestingly, the surface area of the defective NiS/C was found to be lower than NiO/C. However, the enhanced conductivity of the vacancy-rich composite played an important role on improving the electrochemical characteristics. Moreover, this S-vacancy engineering also reduced the contact angle, enhancing the wettability of the electrode, which displayed superior charge storage when compared to NiO/C. In another work, S-vacancy rich MnS nanosheets were directly grown on 3D reduced graphene oxide (rGO) in order to fabricate advanced supercapacitor electrodes with high cycling stability.[119] Herein the crystallinity of the MS has not been degraded, because the S-vacancies were generated at appropriate levels. Helped by both the pseudocapacitive nature of the vacancy-rich MnS and the EDLC characteristics of rGO, the composite electrode exhibited a promising volumetric capacitance of 27.98 F cm^{-3}. Moreover, the electrode also retained 88.5% of its initial capacitance after 5000 cycles. The role of S-vacancies in the improved electrode performance of this composite electrode has been evaluated through DFT analysis. The researchers found that the diffusion barrier has been reduced from 0.31 to 0.19 eV upon the introduction of S-vacancies in MnS. This further improved the transport process of the charge carriers (the electrolyte ions), and also increased the contact area between the electrode and electrolyte. Such S-vacancy engineering has also been extended to other MSs for supercapacitor applications. Some of the more recently reported examples of electrodes based on metal sulphides are CoS,[78] MoS_2,[186,187] CuS,[188] and Ni_3S_4.[189]

Mixed metal sulphides (MMSs) have been considered as having good potential for supercapacitor electrodes due to their stable crystal structure as well as their multiple valencies. As expected, the creation of S-vacancies in such MMSs further enhances their electrochemical performance. As an example, Tao *et al.* reported the growth of S-deficient bimetallic $FeNi_2S_4$ on rGO through a solvothermal approach.[190] The introduction of S-vacancies enhanced the specific capacity of $FeNi_2S_4$/rGO from 637.5 to 746.8 C g^{-1}. The increase in the number of redox active sites through S-vacancies further enhanced the rate capability. In another work, the electrochemical reactivity of $CuCo_2S_4$ was enhanced through S-vacancies, following the conventional $NaBH_4$ reduction treatment.[191] As a consequence of the S-deficiency, a significant increment in surface area (from 67.2 to 99.5 cm^2 g^{-1}) has been observed for hollow $CuCo_2S_4$. Apart from the superior capacitance and rate capability, this vacancy-induced MMS displayed lower ionic diffusion resistance, smaller diffusion time constant, and higher fractional exponent than its pristine MMS counterpart, indicating a faster rate of charge diffusion. The supercapacitive properties of $CuCo_2S_4$ have been further enhanced through simultaneous F-doping and S-vacancies.[76] Owing to the synergistic effects from these two types of defects, the MMS displayed a maximum specific capacity of 2202.7 C g^{-1}. Herein, the S-vacancies generated more impurity states in the forbidden band, whereas the F dopant acted as the electron donor. In this way, the S-vacancies enhanced the conductivity, while F-doping increased the density of free electrons in $CuCo_2S_4$. In another research aimed to maximize the charge storage capability of supercapacitors, defect-induced $CoNi_2S_4$ with a vacancy concentration of 3.125% displayed a maximum specific capacity of 1117 C g^{-1}.[192] Notably, the corresponding asymmetric capacitor (ASC) with activated carbon (AC) as negative electrode exhibited a maximum energy density of 55.4 W h kg^{-1}, with a cycling stability of 80% after 10 000 cycles. It is important to notice that the metallic character of $CoNi_2S_4$ has been changed through the induction of S-vacancies. In a similar work, the dual-defects of P-doping and S-vacancies enhanced the capacitive performance of $NiCo_2S_4$.[193]

Proper control of vacancies is crucial for reaching good electrochemical performance, since inducing an extreme degree of vacancies in the material could trigger high structural deformation. During the charge/discharge processes, such defective electrodes may degrade into amorphous phases with high resistance, hampering device performance. For example, the creation of S vacancies exerted a negative impact on the rate capability and cycling stability of another MMS, $NiCo_2S_4$.[194] Despite it higher initial capacitance, the highly defective $NiCo_2S_4$ has been changed into an amorphous phase (with high resistance) during the consecutive charge/discharge cycles. S-vacancy manipulation has also been studied in other bimetallic sulphides, like Zn–Co sulphide.[195,196] The impact of S vacancies over the electrochemical performance of some MS and MMS is illustrated in Fig. 11a–f.

5.1.3. Other vacancies. Besides oxygen and sulphur, other two VI group elements (Se, Te) have already been studied in compounds where they can generate vacancies. Like the other vacancy defects, Se-vacancies also have the ability to adsorb more electrolyte ions and thus enabling a rich redox kinetics. A recent work have demonstrated the impact of Se-vacancy engineering in $Ni(Co)Se_2/Co(Ni)Se_2$ heterojunctions.[197] Owing to the porous structural features and abundant defects, such Se-vacancy rich heterojunction displayed high rate capability (capacity retention of 60.4% upon increasing the current density by 250 times). From theoretical calculations, the diffusion barrier was found to be lower for this defective heterojunction than its defect-free monometallic and bimetallic counterparts. Moreover, the Se-deficient material also displayed higher OH^- ion adsorption energy than its other counterparts. Benefited by such special characteristics, the defective heterojunction exhibited good cycling stability of 97.7% after 5000 cycles. In another work, S-vacancy induced porous $NiSe_2$ demonstrated higher capacitance (466 F g^{-1}) than defect-free $NiSe_2$ nanosheets (328 F g^{-1}) and $NiSe_2$ particles (251 F g^{-1}).[198] Apart from Se, Te-vacancies also played a vital role in enhancing the electrochemical performance of GaTe nanosheets.[199] Along with the Ga, Te vacancies enhanced the semiconducting characteristics of the nanosheets due to the formation of dangling bonds through defects. As a result, the defect-induced chalcogenide exhibited a high cycling stability of 96% after 10 000 cycles.

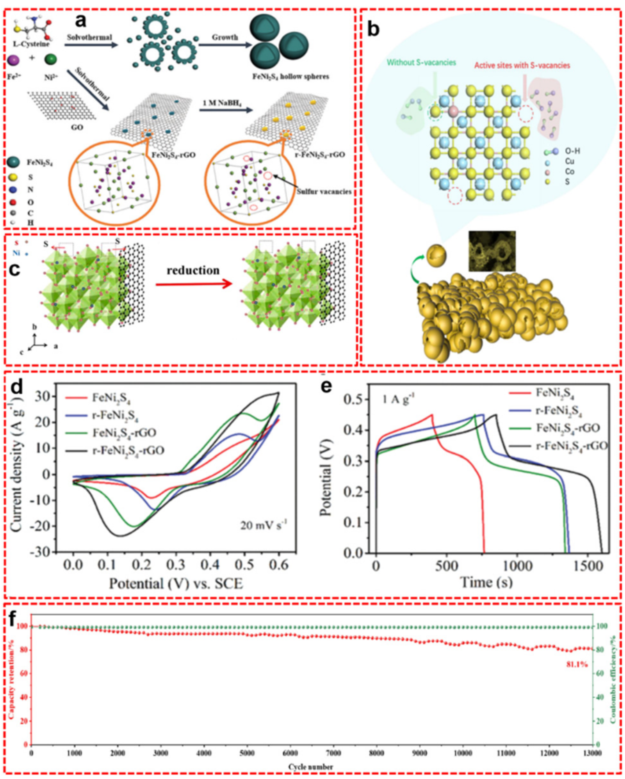

Fig. 11 Sulphur vacancies and their impact on electrochemical properties: (a) synthetic approach for defect-rich $FeNi_2S_4$/rGO composites,[190] (b) schematics illustrating the S-vacancies as the active sites for absorbing OH^- ions in S-vacancy rich $CuCo_2S_4$,[191] (c) mechanism for introducing S-vacancies in NiS through a $NaBH_4$ reduction process[185]; comparative (d) CV curves and (e) GCD plots of $FeNi_2S_4$, defective $FeNi_2S_4$ (r-$FeNi_2S_4$), $FeNi_2S_4$/rGO, and S-deficient $FeNi_2S_4$/rGO (r-$FeNi_2S_4$-rGO),[190] (f) cycling stability of S-vacancy rich $CuCo_2S_4$ over 13 000 cycles.[191] Reproduced with permission from ref. 185, 190, 191 Copyright 2021 & 2022 Elsevier and 2021 Royal Society of Chemistry.

5.2. Secondary batteries

Secondary batteries are another class of energy storage devices which which has drawn significant research interest in the past few years. Owing to their enhanced energy density and good cycle-life, such rechargeable devices have been extensively used in portable electronic appliances. Among the rechargeable batteries, Li-ion batteries (LiBs) are the most popular ones. However, with rapid progress in this field, many other types of batteries like Na-ion, Li-air, Zn-ion, Al-ion, Al-sulphur batteries, *etc.* have been developed.[200–202] Great attention has been paid in the development of such batteries because of their enhanced theoretical capacity as well as their low cost. Vacancy engineering played a vital role on the improvement in battery performance for various electrode materials, including metal oxides/mixed metal oxides, sulphides, hydroxides, *etc.*

5.2.1. Oxygen vacancies. In parallel to the developments in supercapacitor devices, in battery technology oxygen vacancies also played a significant role by improving the redox kinetics, enhancing the conductivity as well as the capacitive characteristics of the metal oxides. In this context, Hou *et al.* demonstrated the formation of vacancy-rich hollow Co_3O_4 microspheres for application in Li batteries.[203] Owing to its mesoporous structure, this oxygen-deficient MO displayed a maximum discharge capacity of 2164.1 mA h g^{-1}. It is noteworthy to mention that the electrode exhibited a capacity of 1307.9 mA h g^{-1} after 1000 cycles. However, vacancy creation through calcination did not alter the crystal structure of Co_3O_4. However, the enhancement in donor density through vacancy generation led to the formation of nonstoichiometric Co_3O_4. The introduction of vacancies generated local in-built electric fields, improving Li-ion storage ability (Fig. 12c). Moreover, the vacancies also promoted Li ion migration during both charging and discharging processes. The unintended creation of oxygen vacancies during charge cycling has a negative effect on the capacity, inducing capacity fading. A recent article has investigated capacity fading, maintaining that in most of the transition metal oxide-based cathode materials, the gradual fading is

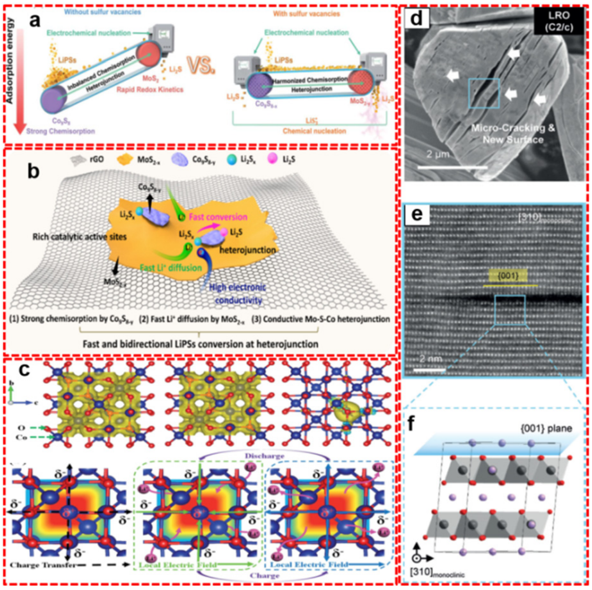

Fig. 12 O and S-vacancies and their impact on battery performance: (a) schematics for the catalytic mechanism of S-vacancy induced heterojunctions for interconversion of LiPSs in Li–S batteries: conventional Co_9S_8/MoS_2 *vs.* Co_9S_{8-x}/MoS_{2-y} heterojunctions,[212] (b) schematics for the catalytic conversion of LiPSs on MoS_{2-x}–Co_9S_{8-y}/rGO heterostructures for Li–S batteries,[211] (c) schematic representation of the mechanism of charge storage through oxygen vacancy derived local built-in electric field in Co_3O_4 for LiBs[203]; (d) SEM image, (e) HAADF-STEM image, and (f) magnified atomic structure of the microcraks formed in Li_2RuO_3-based LiB cathode after electrochemical cycling.[204] Reproduced with permission from ref. 203, 204, 211, 212. Copyright 2018 & 2022 Royal Society of Chemistry, 2022 Elsevier and 2029 Wiley.

caused by the appearance of microcracks generated through the continuous diffusion and accumulation of oxygen vacancies.[204] For Li-based transition metal oxides, such microcraks are generated along the[111] plane of the oxygen sublattice (Fig. 12d–f). Therefore, it is necessary to prevent the diffusion of oxygen vacancies in order to restrict the degradation of the electrode materials. However, Al-doping of Li-based metal oxides can reduce the structural deformation by reducing Mn-ion migration, which can be caused by both the oxygen vacancies and any phase transitions. In another example of the important role played by vacancies, oxygen-deficient N-doped KMn_8O_{16} displayed superior charge storage performance for its application in aqueous Zn-ion batteries.[205] The battery electrode exhibited only 9% capacity fading over 2500 cycles. The theoretical studies confirmed the presence of electrons gathering in the Mn atoms near to oxygen vacancies, and doped N atoms, which indicates strong interaction between Mn, O, and N atoms. Moreover, the diffusion coefficient was found to be higher than for pristine MnO_2, indicating faster ion diffusion. Additionally, the insertion energy of H^+ in the defective KMn_8O_{16} was also calculated to be lower than for MnO_2. Therefore, the dual effect of doping and vacancy formation was found to be beneficial for enhanced cycling performance. In another work, vacancy-induced $NiCoMnO_4$ achieved the capacity retention of 89.3% after 2800 cycles.[206] In this case, the oxygen vacancies significantly restricted the steady dissolution of Mn^{2+}, which prevented fast capacity fading during cycling. Moreover, the electrochemical analysis of the corresponding full cell also displayed lesser surface/plating characteristics, indicating minimal ion diffusion resistance and efficient charge transport behaviour. Apart from these studies, such vacancy strategy has been investigated for other batteries like Zn–air,[207] Li–air,[208] $Li–O_2$ batteries[209] *etc.*

5.2.2. **Sulphur vacancies.** Sulphur vacancy manipulation has been widely employed in electrode materials for Li–S batteries. Sulphur vacancy creation in metal sulphides/mixed metal sulphides results in enhanced charge-transfer kinetics as well as improved catalytic activity. For example, by accelerating the polysulfide conversion kinetics, sulphur-deficient MoS_2/rGO composites displayed a low capacity fading rate of 0.083% per cycle over 600 cycles.[210] The capacity loss has been reduced because the formation of insoluble sulphur products has been avoided. Sulphur vacancies have been simultaneously introduced in both MoS_2 and Co_9S_8 to improve the battery performance of a covalent MoS_2–Co_9S_8 heterostructure, grown on rGO sheets.[211] The formation of Mo–S–Co heterojunction (MoS_{2-x}–Co_9S_{8-y}) in the heterostructure served as an active site for enhancing such batteries (Fig. 12b). By tuning the band gap, the vacancy-induced heterostructure improved the conductivity as well as the bidirectional catalytic activity. As a result, the electrode displayed low capacity fading over 600 cycles (0.06% capacity fading per cycle). It is noteworthy to mention that, compared to Co_9S_{8-y}, MoS_{2-x} displayed a lower Li^+ diffusion barrier, indicating its enhanced Li^+ diffusion kinetics. In another work, the authors demonstrated that the creation of S-vacancies in MoS_2/Co_9S_8 heterojunctions can generate $LiS_3^{\bullet}$ radicals, which further improve the battery performance by reducing the growth of liquid Li polysulfides (LiPSs).[212] In particular, with the S-vacancies, the sulphide heterojunction materials homogeneously absorbed the LiPSs and simplified the conversion of LiPSs to Li_2S (Fig. 12a). Moreover, the S-vacancies also improved the redox kinetics of LiPSs. The S-vacancy engineering strategy was further extended towards other metal sulphides like In_2S_3. A recent publication demonstrated the anchoring role of S-vacancies in a In_2S_{3-x}/rGO composite to promote the conversion of LiPSs.[213] Such vacancies favoured the formation of thiosulfate and polythionate, which strongly absorbed the LiPSs. Overall, such vacancy-induced composite acted as a cathode catalyst, which not only seized polysulfide to restrict the loss of active materials, but also speeded the conversion of polysulfides to prevent its accumulation on the electrode surface. The introduction of S-vacancies has significantly enhanced the catalytic kinetics of VS_2.[160] Owing to the enhancement of coordination unsaturated sites and charge re-distribution, such S-deficient metal sulphide displayed a maximum discharge capacity of 1492.2 mA h g^{-1} and minimal fading rate of 0.07% over 1000 cycles. Such vacancy engineering was further employed to improve the electrochemical performance of Zn-ion batteries. In this context, Lei *et al.* demonstrated the enhanced Zn^{2+} storage capacity of CuS_{1-x}/polyaniline anodes.[214] Herein, the S-vacancies enhanced the surface active sites to improve the storage capacity of Zn^{2+}, while the conductive polyaniline improved ionic conductivity, and restricted the structural deformation upon volume expansion during cycling. Such dual effects are beneficial for not only the capacity enhancement, but also for the improvement in rate capability. Most importantly, the corresponding Zn-ion battery full cell with Zn_xMnO_2 cathode exhibited maximum capacity retention of 80% after 10 000 cycles. In another work, defective MoS_{2-x} was uniformly coated on CNT webs to develop effective cathode catalysts for Li–O_2 batteries.[215] The S-vacancies significantly enhanced the oxygen reduction and evolution reactions. Overall, S-vacancies have demonstrated a positive effect on the electrochemical performance of several types of secondary batteries.

5.2.3. **Other vacancies.** Like the S-vacancies, Se-vacancies also improved the performance of Li–S batteries by restricting the polysulfide shuttling. The introduction of Se-vacancies in Sb_2Se_3/rGO composites enhanced the chemical affinity to LiPSs, yielding devices with a low capacity fading rate of 0.027% per cycle over 500 cycles.[216] In particular, the defective Sb_2Se_{3-x} served as the multifunctional barrier to tackle the issue of slow conversion kinetics in LiPSs. In another work, the authors introduced P-doped $NiTe_2$ electrocatalyst rich in Te vacancies in order to accelerate the redox kinetics of Li–S batteries.[217] The theoretical study demonstrated a lower Li_2S decomposition barrier on the defective $NiTe_2$ when compared to its pristine counterpart, which indicates enhanced Li_2S transformation kinetics as well as improved catalytic activity. As a result, such Te-deficient $NiTe_2$ anchored on maize straw-derived carbon demonstrated an excellent capacity decay rate of 0.0139% per cycle over 1800 cycles. Besides these types of vacancies, P vacancies in CoP have also promoted the diffusion kinetics of Li^+ for its application in Li–S batteries.[218] Like other vacancies, such P vacancies modified the electronic structure of CoP, enhancing the redox kinetics in LiPSs liquid-phase conversion.

6. Conclusions and future perspective

This review article highlighted some of the recent improvements in the performance of energy storage devices (supercapacitors and secondary batteries). The creation of vacancies in 2D materials is considered to be largely responsible for the optimized electrochemical behaviour, highlighting the essential role of defect engineering. Despite the significant experimental effort spent on vacancies creation, vacancy engineering research in 2D materials is still in its development phase, keeping a lot of potential for progress.

Several of the most effective experimental approaches for vacancy creation have already been applied to 2D materials, such as microwave irradiation, ion implantation, ultraviolet irradiation, hydrothermal/solvothermal treatments, high temperature treatments under controlled atmospheres, plasma treatments, liquid phase exfoliation. Notably, there is an essential need for further improvements in a wide range of methodologies for characterizing the vacancy defects, regarding their type, location and concentration in 2D materials. EPR, XPS, XAFS, PAS, Raman spectroscopy, and high-resolution microscopy are some of the best characterization methods that may allow the precise identification and quantification of a wide variety of surface and vacancy defects in 2D materials.

Vacancy defects in 2D electrode materials have a significant impact on the impressive performance records seen in the scientific literature for charge storage devices. By studying the impact of vacancies, researchers have fabricated electrode materials containing oxygen or sulphur vacancies. Their success is widely referred and has been associated to some of the best performing supercapacitors and secondary batteries. Vacancies and surface defects work as active sites to make a positive contribution to the working mechanisms of these devices. It has been proven through theoretical calculations, structural characterization, and electrochemical research that the inclusion of vacancies in 2D materials can improve the charge-transfer properties, as well as the ion diffusion processes, boosting the rate capability by increasing the electronic conductivity, lowering the energy barriers for ion intercalation, and providing additional sites for charge storage in energy storage devices.

In spite of the many developments discussed in this concise review, there are several significant challenges still remaining in the design, synthesis, and application of defective 2D materials. Besides graphene, it is still challenging to synthesize large scale, ultrathin 2D materials having a controlled number of layers over large areas. It is very crucial for researchers in this area to focus on finding solutions related to a better way to characterize vacancies regarding their type, location, and concentration. An even better control over the creation of defects (including vacancies) in 2D materials will surely allow for better energy storage devices in the near future.

Author contributions

Rajesh Kumar and Sumanta Sahoo discussed about the organization and presentation of the contents of this feature article and finally wrote the original draft. Ednan Joanni suggested his idea and participated as reviewing and editing of the feature article. Raghvendra Pandey and Jae-Jin Shim discussed about their view on the presence of vacancies in materials. All authors have given approval to the final version of the feature article.

Conflicts of interest

There are no conflicts to declare.

Acknowledgements

R. Kumar gratefully acknowledges the support of this research by Science and Engineering Research Board (SERB), Department of Science & Technology (DST), New Delhi, India under Ramanujan Fellowship/Award (SB/S2/RJN-159/2017). Also, this research study was supported by the National Research

Foundation (NRF) of the Republic of Korea under the frameworks of the Priority Research Centers Program (NRF-2014R1A6A1031189) and the Regional University Superior Scientist Research Program (NRF-2020R1I1A3073981) funded by the Ministry of Education, the Republic of Korea.

References

1 H. D. Yoo, E. Markevich, G. Salitra, D. Sharon and D. Aurbach, On the challenge of developing advanced technologies for electrochemical energy storage and conversion, *Mater. Today*, 2014, **17**(3), 110–121.
2 X. Tian, J. Jin, S. Yuan, C. K. Chua, S. B. Tor and K. Zhou, Emerging 3D-printed electrochemical energy storage devices: a critical review, *Adv. Energy Mater.*, 2017, **7**(17), 1700127.
3 H. Li, L. Peng, Y. Zhu, X. Zhang and G. Yu, Achieving high-energy–high-power density in a flexible quasi-solid-state sodium ion capacitor, *Nano Lett.*, 2016, **16**(9), 5938–5943.
4 S. Chu, Y. Cui and N. Liu, The path towards sustainable energy, *Nat. Mater.*, 2017, **16**(1), 16–22.
5 H. Ryu, H. J. Yoon and S. W. Kim, Hybrid energy harvesters: toward sustainable energy harvesting, *Adv. Mater.*, 2019, **31**(34), 1802898.
6 R. Walden, C. Kumar, D. M. Mulvihill and S. C. Pillai, Opportunities and challenges in triboelectric nanogenerator (TENG) based sustainable energy generation technologies: a mini-review, *Chem. Eng. J. Adv.*, 2021, 100237.
7 R. Kumar, S. Sahoo, E. Joanni, R. K. Singh, W. K. Tan and A. Matsuda, Recent progress in the synthesis of graphene and derived materials for next generation electrodes of high performance lithium ion batteries, *Prog. Energy Combust. Sci.*, 2019, **75**, 100786.
8 R. Kumar, A. P. del Pino, S. Sahoo, R. K. Singh, W. K. Tan, A. Matsuda and E. Joanni, Laser processing of graphene and related materials for energy storage: State of the art and future prospects, *Prog. Energy Combust. Sci.*, 2022, 100981.
9 S. Sahoo, R. Kumar, E. Joanni, R. K. Singh and J.-J. Shim, Advances in pseudocapacitive and battery-like electrode materials for high performance supercapacitors, *J. Mater. Chem. A*, 2022, **10**(25), 13190–13240.
10 Y. Zhu, S. Wang, J. Ma, P. Das, S. Zheng and Z.-S. Wu, Recent status and future perspectives of 2D MXene for micro-supercapacitors and micro-batteries, *Energy Storage Mater.*, 2022, **51**, 500–526.
11 M. K. Aslam, Y. Niu and M. Xu, MXenes for non-lithium-ion (Na, K, Ca, Mg, and Al) batteries and supercapacitors, *Adv. Energy Mater.*, 2021, **11**(2), 2000681.
12 R. Lakra, R. Kumar, P. K. Sahoo, D. Thatoi and A. Soam, A mini-review: Graphene based composites for supercapacitor application, *Inorg. Chem. Commun.*, 2021, **133**, 108929.
13 I. Hussain, S. Sahoo, T. Hussain, M. Ahmad, M. S. Javed, C. Lamiel, S. Gu, T. Kaewmaraya, M. S. Sayed and K. Zhang, Theoretical and experimental investigation of in situ grown MOF-derived oriented Zr-Mn-oxide and solution-free CuO as hybrid electrode for supercapacitors, *Adv. Funct. Mater.*, 2022, 2210002.
14 L. Li, Z. Xie, G. Jiang, Y. Wang, B. Cao and C. Yuan, Efficient laser-induced construction of oxygen-vacancy abundant nano-$ZnCo_2O_4$/porous reduced graphene oxide hybrids toward exceptional capacitive lithium storage, *Small*, 2020, **16**(32), 2001526.
15 L. Fagiolari, M. Sampò, A. Lamberti, J. Amici, C. Francia, S. Bodoardo and F. Bella, Integrated energy conversion and storage devices: Interfacing solar cells, batteries and supercapacitors, *Energy Storage Mater.*, 2022, **51**, 400–434.
16 Y. Zhang, L. Li, H. Su, W. Huang and X. Dong, Binary metal oxide: advanced energy storage materials in supercapacitors, *J. Mater. Chem. A*, 2015, **3**(1), 43–59.
17 Y. Zhao, X. Li, B. Yan, D. Xiong, D. Li, S. Lawes and X. Sun, Recent developments and understanding of novel mixed transition-metal oxides as anodes in lithium ion batteries, *Adv. Energy Mater.*, 2016, **6**(8), 1502175.
18 R. C. K. Reddy, J. Lin, Y. Chen, C. Zeng, X. Lin, Y. Cai and C.-Y. Su, Progress of nanostructured metal oxides derived from metal–organic frameworks as anode materials for lithium–ion batteries, *Coord. Chem. Rev.*, 2020, **420**, 213434.
19 L. Li, J. Zhang, Y. Wang, F. U. Zaman, Y. Zhang, L. Hou and C. Yuan, Laser irradiation construction of nanomaterials toward electrochemical energy storage and conversion: Ongoing progresses and challenges, *InfoMat*, 2021, **3**(12), 1393–1421.
20 R. Kumar, S. M. Youssry, M. M. Abdel-Galeil and A. Matsuda, One-pot synthesis of reduced graphene oxide nanosheets anchored ZnO nanoparticles *via* microwave approach for electrochemical performance as supercapacitor electrode, *J. Mater. Sci.: Mater. Electron.*, 2020, **31**(18), 15456–15465.
21 Y. Fang, D. Luan and X. W. Lou, Recent advances on mixed metal sulfides for advanced sodium-ion batteries, *Adv. Mater.*, 2020, **32**(42), 2002976.
22 Q. Liu, F. Wang, H. Lin, Y. Xie, N. Tong, J. Lin, X. Zhang, Z. Zhang and X. Wang, Surface oxygen vacancy and defect engineering of WO_3 for improved visible light photocatalytic performance, *Catal. Sci. Technol.*, 2018, **8**(17), 4399–4406.
23 J. Wang, X. Yue, Z. Xie, A. Abudula and G. Guan, MOFs-derived transition metal sulfide composites for advanced sodium ion batteries, *Energy Storage Mater.*, 2021, **41**, 404–426.
24 Y. Gao and L. Zhao, Review on recent advances in nanostructured transition-metal-sulfide-based electrode materials for cathode materials of asymmetric supercapacitors, *Chem. Eng. J.*, 2022, **430**, 132745.
25 R. Kumar, S. M. Youssry, E. Joanni, S. Sahoo, G. Kawamura and A. Matsuda, Microwave-assisted synthesis of iron oxide homogeneously dispersed on reduced graphene oxide for high-performance supercapacitor electrodes, *J. Energy Storage*, 2022, **56**, 105896.
26 R. R. Salunkhe, Y. V. Kaneti and Y. Yamauchi, Metal–organic framework-derived nanoporous metal oxides toward supercapacitor applications: progress and prospects, *ACS Nano*, 2017, **11**(6), 5293–5308.
27 R. Kumar, S. Sahoo, E. Joanni and R. K. Singh, Microwave as a Tool for Synthesis of Carbon-Based Electrodes for Energy Storage, *ACS Appl. Mater. Interfaces*, 2022, **14**(18), 20306–20325.
28 M. Kandasamy, S. Sahoo, S. K. Nayak, B. Chakraborty and C. S. Rout, Recent advances in engineered metal oxide nanostructures for supercapacitor applications: experimental and theoretical aspects, *J. Mater. Chem. A*, 2021, **9**(33), 17643–17700.
29 R. Kumar, S. Sahoo, E. Joanni and R. K. Singh, A review on the current research on microwave processing techniques applied to graphene-based supercapacitor electrodes: An emerging approach beyond conventional heating, *J. Energy Chem.*, 2022, **74**, 252–282.
30 P. Geng, S. Zheng, H. Tang, R. Zhu, L. Zhang, S. Cao, H. Xue and H. Pang, Transition metal sulfides based on graphene for electrochemical energy storage, *Adv. Energy Mater.*, 2018, **8**(15), 1703259.
31 Y. Xiao, S. H. Lee and Y. K. Sun, The application of metal sulfides in sodium ion batteries, *Adv. Energy Mater.*, 2017, **7**(3), 1601329.
32 S. M. Youssry, I. S. El-Hallag, R. Kumar, G. Kawamura, W. K. Tan, A. Matsuda and M. N. El-Nahass, Electrochemical deposition of uniform and porous Co-Ni layered double hydroxide nanosheets on nickel foam for supercapacitor electrode with improved electrochemical efficiency, *J. Energy Storage*, 2022, **50**, 104638.
33 S. M. Youssry, M. N. El-Nahass, R. Kumar, I. S. El-Hallag, W. K. Tan and A. Matsuda, Superior performance of $Ni(OH)_2$-ErGO@NF electrode materials as pseudocapacitance using electrochemical deposition *via* two simple successive steps, *J. Energy Storage*, 2020, **30**, 101485.
34 Y. Hu, W. Lu, L. Yan, W. Ye, J. Ning and Y. Zhong, Defect engineering of electrode materials towards superior reaction kinetics for high-performance supercapacitors, *J. Mater. Chem. A*, 2022, **10**, 15267–15296.
35 Y. Zhang, L. Tao, C. Xie, D. Wang, Y. Zou, R. Chen, Y. Wang, C. Jia and S. Wang, Defect engineering on electrode materials for rechargeable batteries, *Adv. Mater.*, 2020, **32**(7), 1905923.
36 T. Xiong, Y. Zhang, W. S. V. Lee and J. Xue, Defect engineering in manganese-based oxides for aqueous rechargeable zinc-ion batteries: a review, *Adv. Energy Mater.*, 2020, **10**(34), 2001769.
37 J. Qi, Y. Yan, Y. Cai, J. Cao and J. Feng, Nanoarchitectured design of vertical-standing arrays for supercapacitors: progress, challenges, and perspectives, *Adv. Funct. Mater.*, 2021, **31**(3), 2006030.
38 S. Zhang, X. Yi, G. Hu, M. Chen, H. Shen, B. Li, L. Yang, W. Dai, J. Zou and S. Luo, Configuration regulation of active sites by accurate doping inducing self-adapting defect for enhanced photocatalytic applications: A review, *Coord. Chem. Rev.*, 2023, **478**, 214970.
39 Y. Zhang, H. Liu, S. Zhao, C. Xie, Z. Huang and S. Wang, Insights into the dynamic evolution of defects in electrocatalysts, *Adv. Mater.*, 2023, 2209680.

40 J. Liu, M. Zheng, J. Li, Y. Yuan, C. Li, S. Zhang, L. Yang, Z. Bai and J. Lu, Lithiation-induced defect engineering to promote oxygen evolution reaction, *Adv. Funct. Mater.*, 2023, **33**(2), 2209753.
41 Z. Yuan, F. Xiao, Y. Fang, P. Xiong, X. Sun, X. Duan, X. Yang, H. Fan, M. Wei and Q. Qian, Defect engineering on VO_2 (B) nanoleaves/graphene oxide for the high performance of cathodes of zinc-ion batteries with a wide temperature range, *J. Power Sources*, 2023, **559**, 232688.
42 R. Kumar, S. Sahoo, E. Joanni, R. K. Singh, K. Maegawa, W. K. Tan, G. Kawamura and A. Matsuda, Heteroatom doped graphene engineering for energy storage and conversion, *Mater. Today*, 2020, **39**, 47–65.
43 R. Kumar, W. C. Macedo Jr, R. K. Singh, V. S. Tiwari, C. J. L. Constantino, A. Matsuda and S. A. Moshkalev, Nitrogen–sulfur co-doped reduced graphene oxide-nickel oxide nanoparticle composites for electromagnetic interference shielding, *ACS Appl. Nano Mater.*, 2019, **2**(7), 4626–4636.
44 R. Kumar, R. K. Singh and R. S. Tiwari, Growth analysis and high-yield synthesis of aligned-stacked branched nitrogen-doped carbon nanotubes using sesame oil as a natural botanical hydrocarbon precursor, *Mater. Des.*, 2016, **94**, 166–175.
45 R. Kumar, S. Sahoo, E. Joanni, R. K. Singh, W. K. Tan, S. A. Moshkalev and A. Matsuda, Heteroatom doping of 2D graphene materials for electromagnetic interference shielding: a review of recent progress, *Crit. Rev. Solid State Mater. Sci.*, 2022, **47**(4), 570–619.
46 G. Li, G. R. Blake and T. T. Palstra, Vacancies in functional materials for clean energy storage and harvesting: the perfect imperfection, *Chem. Soc. Rev.*, 2017, **46**(6), 1693–1706.
47 P. Gao, Z. Chen, Y. Gong, R. Zhang, H. Liu, P. Tang, X. Chen, S. Passerini and J. Liu, The role of cation vacancies in electrode materials for enhanced electrochemical energy storage: synthesis, advanced characterization, and fundamentals, *Adv. Energy Mater.*, 2020, **10**(14), 1903780.
48 Y. Liu, C. Xiao, Z. Li and Y. Xie, Vacancy engineering for tuning electron and phonon structures of two-dimensional materials, *Adv. Energy Mater.*, 2016, **6**(23), 1600436.
49 S. A. Morin and S. Jin, Screw dislocation-driven epitaxial solution growth of ZnO nanowires seeded by dislocations in GaN substrates, *Nano Lett.*, 2010, **10**(9), 3459–3463.
50 Q. Zhang, J. Wang, D. Xu, Z. Wang, X. Li and K. Zhang, Facile large-scale synthesis of vertically aligned CuO nanowires on nickel foam: growth mechanism and remarkable electrochemical performance, *J. Mater. Chem. A*, 2014, **2**(11), 3865–3874.
51 J. A. Dawson and I. Tanaka, Li intercalation into a β-MnO_2 grain boundary, *ACS Appl. Mater. Interfaces*, 2015, **7**(15), 8125–8131.
52 X. Sun, Z. Wang and Y. Q. Fu, Defect-mediated lithium adsorption and diffusion on monolayer molybdenum disulfide, *Sci. Rep.*, 2015, **5**(1), 1–9.
53 Y. Sun, Q. Liu, S. Gao, H. Cheng, F. Lei, Z. Sun, Y. Jiang, H. Su, S. Wei and Y. Xie, Pits confined in ultrathin cerium (IV) oxide for studying catalytic centers in carbon monoxide oxidation, *Nat. Commun.*, 2013, **4**(1), 2899.
54 V. Amoli, S. Bhat, A. Maurya, B. Banerjee, A. Bhaumik and A. K. Sinha, Tailored synthesis of porous TiO_2 nanocubes and nanoparallelepipeds with exposed {111} facets and mesoscopic void space: A superior candidate for efficient dye-sensitized solar cells, *ACS Appl. Mater. Interfaces*, 2015, **7**(47), 26022–26035.
55 F. Lei, Y. Sun, K. Liu, S. Gao, L. Liang, B. Pan and Y. Xie, Oxygen vacancies confined in ultrathin indium oxide porous sheets for promoted visible-light water Splitting, *J. Am. Chem. Soc.*, 2014, **136**(19), 6826–6829.
56 N. Zhang, Z. Xing, Z. Li and W. Zhou, Sulfur vacancy engineering of metal sulfide photocatalysts for solar energy conversion, *Chem. Catal.*, 2022, 100375.
57 C. Liu, C. Zhang, H. Song, X. Nan, H. Fu and G. Cao, MnO nanoparticles with cationic vacancies and discrepant crystallinity dispersed into porous carbon for Li-ion capacitors, *J. Mater. Chem. A*, 2016, **4**(9), 3362–3370.
58 W. Li, D. Corradini, M. Body, C. Legein, M. Salanne, J. Ma, K. W. Chapman, P. J. Chupas, A.-L. Rollet and C. Julien, High substitution rate in TiO_2 anatase nanoparticles with cationic vacancies for fast lithium storage, *Chem. Mater.*, 2015, **27**(14), 5014–5019.
59 M. Pernet, P. Strobel, B. Bonnet, P. Bordet and Y. Chabre, Structural and electrochemical study of lithium insertion into γ-Fe_2O_3, *Solid State Ionics*, 1993, **66**(3–4), 259–265.
60 G. Huang, Y. Yang, H. Sun, S. Xu, J. Wang, M. Ahmad and Z. Xu, Defective $ZnCo_2O_4$ with Zn vacancies: synthesis, property and electrochemical application, *J. Alloys Compd.*, 2017, **724**, 1149–1156.
61 P. K. Dubey, R. Kumar, R. S. Tiwari, O. N. Srivastava, A. C. Pandey and P. Singh, Surface modification of aligned TiO_2 nanotubes by Cu_2O nanoparticles and their enhanced photo electrochemical properties and hydrogen generation application, *Int. J. Hydrogen Energy*, 2018, **43**(14), 6867–6878.
62 I. Persson, A. El Ghazaly, Q. Tao, J. Halim, S. Kota, V. Darakchieva, J. Palisaitis, M. W. Barsoum, J. Rosen and P. O. Persson, Tailoring structure, composition, and energy storage properties of MXenes from selective etching of in-plane, chemically ordered MAX phases, *Small*, 2018, **14**(17), 1703676.
63 J. Halim, J. Palisaitis, J. Lu, J. Thörnberg, E. Moon, M. Precner, P. Eklund, P. Å. Persson, M. Barsoum and J. Rosen, Synthesis of two-dimensional Nb1.33C (MXene) with randomly distributed vacancies by etching of the quaternary solid solution (Nb2/3Sc1/3) 2AlC MAX phase, *ACS Appl. Nano Mater.*, 2018, **1**(6), 2455–2460.
64 C. Mao, J. Wang, Y. Zou, H. Li, G. Zhan, J. Li, J. Zhao and L. Zhang, Anion (O, N, C, and S) vacancies promoted photocatalytic nitrogen fixation, *Green Chem.*, 2019, **21**(11), 2852–2867.
65 L. Fu, S. Zhou, M. Xiang, J. Yang, W. Fan, Z. Yang and J. Ou, Advances in anion vacancy for electrocatalytic oxygen evolution reaction, *J. Electroanal. Chem.*, 2022, 116650.
66 A. Zhang, R. Gao, L. Hu, X. Zang, R. Yang, S. Wang, S. Yao, Z. Yang, H. Hao and Y.-M. Yan, Rich bulk oxygen vacancies-engineered MnO_2 with enhanced charge transfer kinetics for supercapacitor, *Chem. Eng. J.*, 2021, **417**, 129186.
67 V. Babentsov and R. James, Anion vacancies in II–VI chalcogenides: Review and critical analysis, *J. Cryst. Grow.*, 2013, **379**, 21–27.
68 Y. Ma, B. Qiu, J. Zhang and M. Xing, Vacancy engineering of ultrathin 2D materials for photocatalytic CO_2 reduction, *ChemNanoMat*, 2021, **7**(4), 368–379.
69 A. Zywietz, J. Furthmüller and F. Bechstedt, Neutral vacancies in group-IV semiconductors, *Phys. Status Solidi B*, 1998, **210**(1), 13–29.
70 C. Clark, J. Walker and R. W. Ditchburn, The neutral vacancy in diamond, *Proc. R. Soc. London, Ser. A*, 1973, **334**(1597), 241–257.
71 Y. Wang, Y. Zhang, Z. Liu, C. Xie, S. Feng, D. Liu, M. Shao and S. Wang, Layered double hydroxide nanosheets with multiple vacancies obtained by dry exfoliation as highly efficient oxygen evolution electrocatalysts, *Angew. Chem., Int. Ed.*, 2017, **56**(21), 5867–5871.
72 R. Liu, Y. Wang, D. Liu, Y. Zou and S. Wang, Water-plasma-enabled exfoliation of ultrathin layered double hydroxide nanosheets with multivacancies for water oxidation, *Adv. Mater.*, 2017, **29**(30), 1701546.
73 Y. Wang, S. Tao, H. Lin, G. Wang, K. Zhao, R. Cai, K. Tao, C. Zhang, M. Sun and J. Hu, Atomically targeting NiFe LDH to create multivacancies for OER catalysis with a small organic anchor, *Nano Energy*, 2021, **81**, 105606.
74 Y. Dou, C.-T. He, L. Zhang, H. Yin, M. Al-Mamun, J. Ma and H. Zhao, Approaching the activity limit of $CoSe_2$ for oxygen evolution *via* Fe doping and Co vacancy, *Nat. Commun.*, 2020, **11**(1), 1664.
75 S. Wei, C. Wan, L. Zhang, X. Liu, W. Tian, J. Su, W. Cheng and Y. Wu, N-doped and oxygen vacancy-rich $NiCo_2O_4$ nanograss for supercapacitor electrode, *Chem. Eng. J.*, 2022, **429**, 132242.
76 L. Kang, C. Huang, J. Zhang, M. Zhang, N. Zhang, S. Liu, Y. Ye, C. Luo, Z. Gong and C. Wang, Effect of fluorine doping and sulfur vacancies of $CuCo_2S_4$ on its electrochemical performance in supercapacitors, *Chem. Eng. J.*, 2020, **390**, 124643.
77 Z. Wang, R. Lin, Y. Huo, H. Li and L. Wang, Formation, detection, and function of oxygen vacancy in metal oxides for solar energy conversion, *Adv. Funct. Mater.*, 2022, **32**(7), 2109503.
78 Q. Wang, Z. Qu, S. Chen and D. Zhang, Metal organic framework derived P-doping CoS@ C with sulfide defect to boost high-performance asymmetric supercapacitors, *J. Colloid Interface Sci.*, 2022, **624**, 385–393.
79 R. Kumar, R. K. Singh, P. K. Dubey, D. P. Singh and R. M. Yadav, Self-assembled hierarchical formation of conjugated 3D cobalt oxide nanobead–CNT–graphene nanostructure using microwaves for high-performance supercapacitor electrode, *ACS Appl. Mater. Interfaces*, 2015, **7**(27), 15042–15051.

80 R. K. Singh, R. Kumar, D. P. Singh, R. Savu and S. A. Moshkalev, Progress in microwave-assisted synthesis of quantum dots (graphene/carbon/semiconducting) for bioapplications: a review, *Mater. Today Chem.*, 2019, **12**, 282–314.
81 R. Kumar, S. M. Youssry, K. Z. Ya, W. K. Tan, G. Kawamura and A. Matsuda, Microwave-assisted synthesis of Mn_3O_4–Fe_2O_3/Fe_3O_4@rGO ternary hybrids and electrochemical performance for supercapacitor electrode, *Diamond Relat. Mater.*, 2020, **101**, 107622.
82 R. Kumar, R. K. Singh, R. Savu, P. K. Dubey, P. Kumar and S. A. Moshkalev, Microwave-assisted synthesis of void-induced graphene-wrapped nickel oxide hybrids for supercapacitor applications, *RSC Adv.*, 2016, **6**(32), 26612–26620.
83 R. Kumar, S. Sahoo, W. K. Tan, G. Kawamura and A. Matsuda, Microwave-assisted thin reduced graphene oxide-cobalt oxide nanoparticles as hybrids for electrode materials in supercapacitor, *J. Energy Storage*, 2021, **40**, 102724.
84 R. Kumar, R. K. Singh, A. V. Alaferdov and S. A. Moshkalev, Rapid and controllable synthesis of Fe_3O_4 octahedral nanocrystals embedded-reduced graphene oxide using microwave irradiation for high performance lithium-ion batteries, *Electrochim. Acta*, 2018, **281**, 78–87.
85 R. Kumar, E. T. S. G. da Silva, R. K. Singh, R. Savu, A. V. Alaferdov, L. C. Fonseca, L. C. Carossi, A. Singh, S. Khandka, O. L. Alves, L. T. Kubota and S. A. Moshkalev, Microwave-assisted synthesis of palladium nanoparticles intercalated nitrogen doped reduced graphene oxide and their electrocatalytic activity for direct-ethanol fuel cells, *J. Colloid Interface Sci.*, 2018, **515**, 160–171.
86 R. Kumar, M. M. Abdel-Galeil, K. Z. Ya, K. Fujita, W. K. Tan and A. Matsuda, Facile and fast microwave-assisted formation of reduced graphene oxide-wrapped manganese cobaltite ternary hybrids as improved supercapacitor electrode material, *Appl. Surf. Sci.*, 2019, **481**, 296–306.
87 H. Hashtroudi, R. Kumar, R. Savu, S. Moshkalev, G. Kawamura, A. Matsuda and M. Shafiei, Hydrogen gas sensing properties of microwave-assisted 2D Hybrid Pd/rGO: Effect of temperature, humidity and UV illumination, *Int. J. Hydrogen Energy*, 2021, **46**(10), 7653–7665.
88 R. Kumar, R. K. Singh, D. P. Singh, R. Savu and S. A. Moshkalev, Microwave heating time dependent synthesis of various dimensional graphene oxide supported hierarchical ZnO nanostructures and its photoluminescence studies, *Mater. Des.*, 2016, **111**, 291–300.
89 Z. Cheng, X. Zhang, H. Zhang, H. Liu, X. Yu, X. Dai, G. Liu and G. Chen, Large vacancy-defective graphene for enhanced lithium storage, *Carbon Trends*, 2023, **10**, 100237.
90 C. Wang, Y. Fang, H. Duan, G. Liang, W. Li, D. Chen and M. Long, DFT study of CO_2 adsorption properties on pristine, vacancy and doped graphenes, *Solid State Commun.*, 2021, **337**, 114436.
91 H. Liu, L. Duan, K. Xia, Y. Chen, Y. Li, S. Deng, J. Xu and Z. Hou, Microwave synthesized 2D WO_3 nanosheets for VOCs gas sensors, *Nanomaterials*, 2022, **12**(18), 3211.
92 R. Kumar, J.-H. Oh, H.-J. Kim, J.-H. Jung, C.-H. Jung, W. G. Hong, H.-J. Kim, J.-Y. Park and I.-K. Oh, Nanohole-structured and palladium-embedded 3D porous graphene for ultrahigh hydrogen storage and CO oxidation multifunctionalities, *ACS Nano*, 2015, **9**(7), 7343–7351.
93 H. Wang, J. Tian, L. Guo, X. Guo, Z. Yan, J. Zheng, Q. Feng, W. Zhou and J. Xue, Computational study of low-energy Pt-ion implantation into graphene for single-atom catalysis, *ACS Appl. Nano Mater.*, 2022, **5**(6), 8583–8593.
94 Z. Sun, S. Fang and Y. H. Hu, 3D graphene materials: From understanding to design and synthesis control, *Chem. Rev.*, 2020, **120**(18), 10336–10453.
95 D. Fuchs, B. C. Bayer, T. Gupta, G. L. Szabo, R. A. Wilhelm, D. Eder, J. C. Meyer, S. Steiner and B. Gollas, Electrochemical behavior of graphene in a deep eutectic solvent, *ACS Appl. Mater. Interfaces*, 2020, **12**(36), 40937–40948.
96 S. Kimt, S. Jung, J. Lee, S. Kim and A. G. Fedorov, High-resolution three-dimensional sculpting of two-dimensional graphene oxide by E-beam direct write, *ACS Appl. Mater. Interfaces*, 2020, **12**(35), 39595–39601.
97 K.-M. Yam, N. Guo, Z. Jiang, S. Li and C. Zhang, Enhancing reactivity of SiC-supported graphene by engineering intercalated metal atoms at the interface, *J. Phys. Chem. C*, 2020, **124**(33), 18126–18131.
98 J. Zhang, K. Jia, Y. Huang, Y. Wang, N. Liu, Y. Chen, X. Liu, X. Liu, Y. Zhu, L. Zheng, H. Chen, F. Liang, M. Zhang, X. Duan, H. Wang, L. Lin, H. Peng and Z. Liu, Hydrophilic, clean graphene for cell culture and cryo-EM imaging, *Nano Lett.*, 2021, **21**(22), 9587–9593.
99 S. Nalamati, S. Devkota, J. Li, R. Lavelle, B. Huet, D. Snyder, A. Penn, R. Garcia, L. Reynolds Jr. and S. Iyer, Hybrid GaAsSb/GaAs heterostructure core–shell nanowire/graphene and photodetector applications, *ACS Appl. Electron. Mater.*, 2020, **2**(10), 3109–3120.
100 W. Zhang and A. C. T. Van Duin, Atomistic-scale simulations of the graphene growth on a silicon carbide substrate using thermal decomposition and chemical vapor deposition, *Chem. Mater.*, 2020, **32**(19), 8306–8317.
101 R. Villarreal, P.-C. Lin, Z. Zarkua, H. Bana, H.-C. Tsai, M. Auge, F. Junge, H. Hofsäss, E. Tosi, S. De Feyter, S. De Gendt, S. Brems, E. H. Å hlgren and L. M. C. Pereira, Bond defects in graphene created by ultralow energy ion implantation, *Carbon*, 2023, **203**, 590–600.
102 C. Du, S. Zhao, X. Tang, Q. Yu, F. Gao, Y. Zhou, J. Liu and H. Yi, Synthesis of ultra-thin 2D MnO_2 nanosheets rich in oxygen vacancy defects and the catalytic oxidation of n-heptane, *Appl. Surf. Sci.*, 2022, **606**, 154846.
103 X. Jiao, Z. Chen, X. Li, Y. Sun, S. Gao, W. Yan, C. Wang, Q. Zhang, Y. Lin, Y. Luo and Y. Xie, Defect-mediated electron–hole separation in one-unit-cell $ZnIn_2S_4$ layers for boosted solar-driven CO_2 reduction, *J. Am. Chem. Soc.*, 2017, **139**(22), 7586–7594.
104 S. Ur Rehmanm, J. Liu, Z. Fang, J. Wang, R. Ahmed, C. Wang and H. Bi, Heterostructured TiO_2/C/Co from ZIF-67 frameworks for microwave-absorbing nanomaterials, *ACS Appl. Nano Mater.*, 2019, **2**(7), 4451–4461.
105 E. Kim, J. Hong, S. Hong, C. Kanade, H. Seok, H.-U. Kim and T. Kim, Improvement of oxide removal rate in chemical mechanical polishing by forming oxygen vacancy in ceria abrasives *via* ultraviolet irradiation, *Mater. Chem. Phys.*, 2021, **273**, 124967.
106 L. Ye, L. Zan, L. Tian, T. Peng and J. Zhang, The {001} facets-dependent high photoactivity of BiOCl nanosheets, *Chem. Commun.*, 2011, **47**(24), 6951–6953.
107 K. Zhao, L. Zhang, J. Wang, Q. Li, W. He and J. J. Yin, Surface structure-dependent molecular oxygen activation of BiOCl single-crystalline nanosheets, *J. Am. Chem. Soc.*, 2013, **135**(42), 15750–15753.
108 L. Ye, K. Deng, F. Xu, L. Tian, T. Peng and L. Zan, Increasing visible-light absorption for photocatalysis with black BiOCl, *Phys. Chem. Chem. Phys.*, 2012, **14**(1), 82–85.
109 R. Wu, J. Zhang, Y. Shi, D. Liu and B. Zhang, Metallic WO_2–carbon mesoporous nanowires as highly efficient electrocatalysts for hydrogen evolution reaction, *J. Am. Chem. Soc.*, 2015, **137**(22), 6983–6986.
110 M.-Q. Cao, T.-T. Liu, Y.-H. Zhu, J.-C. Shu and M.-S. Cao, Developing electromagnetic functional materials for green building, *J. Build. Eng.*, 2022, **45**, 103496.
111 W. Tu, Y. Xu, J. Wang, B. Zhang, T. Zhou, S. Yin, S. Wu, C. Li, Y. Huang, Y. Zhou, Z. Zou, J. Robertson, M. Kraft and R. Xu, Investigating the role of tunable nitrogen vacancies in graphitic carbon nitride nanosheets for efficient visible-light-driven H_2 evolution and CO_2 reduction, *ACS Sustainable Chem. Eng.*, 2017, **5**(8), 7260–7268.
112 C.-j Liu, G. P. Vissokov and B. W. L. Jang, Catalyst preparation using plasma technologies, *Catal. Today*, 2002, **72**(3), 173–184.
113 D. Wang, Y. Zou, L. Tao, Y. Zhang, Z. Liu, S. Du, S. Zang and S. Wang, Low-temperature plasma technology for electrocatalysis, *Chin. Chem. Lett.*, 2019, **30**(4), 826–838.
114 K. Jiang, L. Zhu, Z. Wang, K. Liu, H. Li, J. Hu, H. Pan, J. Fu, N. Zhang, X. Qiu and M. Liu, Plasma-treatment induced H_2O dissociation for the enhancement of photocatalytic CO_2 reduction to CH_4 over graphitic carbon nitride, *Appl. Surf. Sci.*, 2020, **508**, 145173.
115 L. Xu, Q. Jiang, Z. Xiao, X. Li, J. Huo, S. Wang and L. Dai, Plasma-engraved Co_3O_4 nanosheets with oxygen vacancies and high surface area for the oxygen evolution reaction, *Angew. Chem., Int. Ed.*, 2016, **55**(17), 5277–5281.

116 H. Li, C. Tsai, A. L. Koh, L. Cai, A. W. Contryman, A. H. Fragapane, J. Zhao, H. S. Han, H. C. Manoharan, F. Abild-Pedersen, J. K. Nørskov and X. Zheng, Activating and optimizing MoS_2 basal planes for hydrogen evolution through the formation of strained sulphur vacancies, *Nat. Mater.*, 2016, **15**(1), 48–53.
117 X. Zhu, S. Huang, Q. Yu, Y. She, J. Yang, G. Zhou, Q. Li, X. She, J. Deng, H. Li and H. Xu, In-situ hydroxyl modification of monolayer black phosphorus for stable photocatalytic carbon dioxide conversion, *Appl. Catal., B*, 2020, **269**, 118760.
118 H. Yu, H. Huang, K. Xu, W. Hao, Y. Guo, S. Wang, X. Shen, S. Pan and Y. Zhang, Liquid-phase exfoliation into monolayered BiOBr nanosheets for photocatalytic oxidation and reduction, *ACS Sustainable Chem. Eng.*, 2017, **5**(11), 10499–10508.
119 J. Di, C. Chen, C. Zhu, P. Song, J. Xiong, M. Ji, J. Zhou, Q. Fu, M. Xu, W. Hao, J. Xia, S. Li, H. Li and Z. Liu, Bismuth vacancy-tuned bismuth oxybromide ultrathin nanosheets toward photocatalytic CO_2 reduction, *ACS Appl. Mater. Interfaces*, 2019, **11**(34), 30786–30792.
120 Z. Luo, R. Miao, T. D. Huan, I. M. Mosa, A. S. Poyraz, W. Zhong, J. E. Cloud, D. A. Kriz, S. Thanneeru, J. He, Y. Zhang, R. Ramprasad and S. L. Suib, Mesoporous MoO_{3-x} material as an efficient electrocatalyst for hydrogen evolution reactions, *Adv. Energy Mater.*, 2016, **6**(16), 1600528.
121 L. Yan, L. Zong, Z. Zhang, J. Li, H. Wu, Z. Cui and J. Kang, Oxygen vacancies activated porous MnO/graphene submicron needle arrays for high-capacity lithium-ion batteries, *Carbon*, 2022, **190**, 402–411.
122 A. Shen, Y. Zou, Q. Wang, R. A. W. Dryfe, X. Huang, S. Dou, L. Dai and S. Wang, Oxygen reduction reaction in a droplet on graphite: Direct evidence that the edge is more active than the basal plane, *Angew. Chem., Int. Ed.*, 2014, **53**(40), 10804–10808.
123 Y. Zhu, Q. Ling, Y. Liu, H. Wang and Y. Zhu, Photocatalytic performance of $BiPO_4$ nanorods adjusted *via* defects, *Appl. Catal., B*, 2016, **187**, 204–211.
124 F. Bai, L. Xu, X. Zhai, X. Chen and W. Yang, Vacancy in ultrathin 2D nanomaterials toward sustainable energy application, *Adv. Energy Mater.*, 2020, **10**(11), 1902107.
125 A. I. Shames, G. G. Zegrya, D. M. Samosvat, V. Y. Osipov and A. Y. Vul, Size effect in electron paramagnetic resonance spectra of impurity centers in diamond particles, *Phys. E*, 2023, **146**, 115523.
126 B. Wang, A. J. Fielding and R. A. W. Dryfe, Electron paramagnetic resonance as a structural tool to study graphene oxide: Potential dependence of the EPR response, *J. Phys. Chem. C*, 2019, **123**(36), 22556–22563.
127 B. Wang, A. J. Fielding and R. A. W. Dryfe, Electron paramagnetic resonance investigation of the structure of graphene oxide: pH-dependence of the spectroscopic response, *ACS Appl. Nano Mater.*, 2019, **2**(1), 19–27.
128 J. Ru, Y. Fan, W. Zhou, Z. Zhou, T. Wang, R. Liu, J. Yang, X. Lu, J. Wang, C. Ji, L. Wang and W. Jiang, Electrically conductive and mechanically strong graphene/mullite ceramic composites for high-performance electromagnetic interference shielding, *ACS Appl. Mater. Interfaces*, 2018, **10**(45), 39245–39256.
129 F. Fu, H. Shen, X. Sun, W. Xue, A. Shoneye, J. Ma, L. Luo, D. Wang, J. Wang and J. Tang, Synergistic effect of surface oxygen vacancies and interfacial charge transfer on Fe(III)/Bi_2MoO_6 for efficient photocatalysis, *Appl. Catal., B*, 2019, **247**, 150–162.
130 E. Serwicka, ESR study on the interaction of water vapour with polycrystalline TiO_2 under illumination, *Colloids Surf.*, 1985, **13**, 287–293.
131 P. F. Cornaz, J. H. C. van Hooff, F. J. Pluijm and G. C. A. Schuit, Surface co-ordination of oxygen on oxygen-deficient TiO_2 and MoO_3 as revealed by ESR-measurements, *Discuss. Faraday Soc.*, 1966, **41**(0), 290–304.
132 C. Naccache, P. Meriaudeau, M. Che and A. J. Tench, Identification of oxygen species adsorbed on reduced titanium dioxide, *Trans. Faraday Soc.*, 1971, **67**(0), 506–512.
133 H. Li, J. Shi, K. Zhao and L. Zhang, Sustainable molecular oxygen activation with oxygen vacancies on the {001} facets of BiOCl nanosheets under solar light, *Nanoscale*, 2014, **6**(23), 14168–14173.
134 B. P. Mishra, L. Acharya, S. Subudhi and K. Parida, Oxygen vacancy rich α-MnO_2 @B/O-g-C_3N_4 photocatalyst: A thriving 1D-2D surface interaction effective towards photocatalytic O2 and H2 evolution through Z-scheme charge dynamics, *Int. J. Hydrogen Energy*, 2022, **47**(75), 32107–32120.
135 X. Wang, X. Yao, H. Bai and Z. Zhang, Oxygen vacancy-rich 2D GO/BiOCl composite materials for enhanced photocatalytic performance and semiconductor energy band theory research, *Environ. Res.*, 2022, **212**, 113442.
136 S. Hu, L. Jin, W. Si, B. Wang and M. Zhu, Sulfur vacancies enriched 2D $ZnIn_2S_4$ nanosheets for improving photoelectrochemical performance, *Catalysts*, 2022, **12**(4), 400.
137 M. A. Denecke, Actinide speciation using X-ray absorption fine structure spectroscopy, *Coord. Chem. Rev.*, 2006, **250**(7), 730–754.
138 S. R. Sutton, A. Lanzirotti, M. Newville, M. D. Dyar and J. Delaney, Oxybarometry and valence quantification based on microscale X-ray absorption fine structure (XAFS) spectroscopy of multivalent elements, *Chem. Geol.*, 2020, **531**, 119305.
139 K. Amezawa, X-ray absorption spectroscopic studies on solid oxide fuel cells and proton-conducting ceramic fuel cells, *Curr. Opin. Electrochem.*, 2020, **21**, 250–256.
140 T. Masuda and T. Kondo, New sights into the electrochemical interface provided by in situ X-ray absorption fine structure and surface X-ray scattering, *Curr. Opin. Electrochem.*, 2019, **14**, 81–88.
141 F. Tuomisto and I. Makkonen, Defect identification in semiconductors with positron annihilation: Experiment and theory, *Rev. Mod. Phys.*, 2013, **85**(4), 1583–1631.
142 Z. Li, C. Xiao, S. Fan, Y. Deng, W. Zhang, B. Ye and Y. Xie, Dual vacancies: An effective strategy realizing synergistic optimization of thermoelectric property in BiCuSeO, *J. Am. Chem. Soc.*, 2015, **137**(20), 6587–6593.
143 Y. Liu, H. Cheng, M. Lyu, S. Fan, Q. Liu, W. Zhang, Y. Zhi, C. Wang, C. Xiao, S. Wei, B. Ye and Y. Xie, Low overpotential in vacancy-rich ultrathin $CoSe_2$ nanosheets for water oxidation, *J. Am. Chem. Soc.*, 2014, **136**(44), 15670–15675.
144 Y. Zhao, G. Chen, T. Bian, C. Zhou, G. I. N. Waterhouse, L.-Z. Wu, C.-H. Tung, L. J. Smith, D. O'Hare and T. Zhang, Defect-rich ultrathin ZnAl-layered double hydroxide nanosheets for efficient photoreduction of CO_2 to CO with water, *Adv. Mater.*, 2015, **27**(47), 7824–7831.
145 P. F. Liu, S. Yang, B. Zhang and H. G. Yang, Defect-rich ultrathin cobalt–iron layered double hydroxide for electrochemical overall water splitting, *ACS Appl. Mater. Interfaces*, 2016, **8**(50), 34474–34481.
146 X. Jiang, Y. Zhang, J. Jiang, Y. Rong, Y. Wang, Y. Wu and C. Pan, Characterization of oxygen vacancy associates within hydrogenated TiO_2: A positron annihilation study, *J. Phys. Chem. C*, 2012, **116**(42), 22619–22624.
147 M. Guan, C. Xiao, J. Zhang, S. Fan, R. An, Q. Cheng, J. Xie, M. Zhou, B. Ye and Y. Xie, Vacancy associates promoting solar-driven photocatalytic activity of ultrathin bismuth oxychloride nanosheets, *J. Am. Chem. Soc.*, 2013, **135**(28), 10411–10417.
148 X. Cong, X.-L. Liu, M.-L. Lin and P.-H. Tan, Application of Raman spectroscopy to probe fundamental properties of two-dimensional materials, *npj 2D Mater. Appl.*, 2020, **4**(1), 13.
149 M. Park, J. S. Choi, L. Yang and H. Lee, Raman spectra shift of few-layer IV-VI 2D materials, *Sci. Rep.*, 2019, **9**(1), 19826.
150 R. Kumar, R. K. Singh, A. K. Singh, A. R. Vaz, C. S. Rout and S. A. Moshkalev, Facile and single step synthesis of three dimensional reduced graphene oxide-$NiCoO_2$ composite using microwave for enhanced electron field emission properties, *Appl. Surf. Sci.*, 2017, **416**, 259–265.
151 R. Kumar, R. K. Singh, J. Singh, R. S. Tiwari and O. N. Srivastava, Synthesis, characterization and optical properties of graphene sheets-ZnO multipod nanocomposites, *J. Alloys Compd.*, 2012, **526**, 129–134.
152 Z. Wu and Z. Ni, Spectroscopic investigation of defects in two-dimensional materials, *Nanophotonics*, 2017, **6**(6), 1219–1237.
153 R. Ge, X. Wu, L. Liang, S. M. Hus, Y. Gu, E. Okogbue, H. Chou, J. Shi, Y. Zhang, S. K. Banerjee, Y. Jung, J. C. Lee and D. Akinwande, A library of atomically thin 2D materials featuring the conductive-point resistive switching phenomenon, *Adv. Mater.*, 2021, **33**(7), 2007792.
154 S. Zhao, M. Lu, S. Xue, L. Yan, P. Miao, Y. Hang, X. Wang, Z. Liu, Y. Wang and L. Tao, A Se Vacancy induced localized Raman mode in two-dimensional $MoSe_2$ grown by CVD, *arXiv*, 2019, preprint, arXiv:1904.09789, DOI: **10.48550/arXiv.1904.09789**.
155 M. Abd Elkodous, G. S. El-Sayyad, M. I. A. Abdel Maksoud, R. Kumar, K. Maegawa, G. Kawamura, W. K. Tan and A. Matsuda, Nanocomposite matrix conjugated with carbon nanomaterials for

photocatalytic wastewater treatment, *J. Hazard. Mater.*, 2021, **410**, 124657.
156 C. Jin, F. Lin, K. Suenaga and S. Iijima, Fabrication of a free-standing boron nitride single layer and its defect assignments, *Phys. Rev. Lett.*, 2009, **102**(19), 195505.
157 S. Singal, A. Joshi, A. K. Tomar, V. Sahu, G. Singh and R. K. Sharma, Vacancies and edges: Enhancing supercapacitive performance metrics of electrode materials, *J. Energy Storage*, 2020, **31**, 101614.
158 J. Shen, P. Wang, H. Jiang, H. Wang, B. G. Pollet, R. Wang and S. Ji, MOF derived graphitic carbon nitride/oxygen vacancies-rich zinc oxide nanocomposites with enhanced supercapacitive performance, *Ionics*, 2020, **26**(10), 5155–5165.
159 Q. Ma, F. Cui, J. Zhang, X. Qi and T. Cui, Surface engineering of Co_3O_4 nanoribbons forming abundant oxygen-vacancy for advanced supercapacitor, *Appl. Surf. Sci.*, 2022, **578**, 152001.
160 Y. Wu, Y. Wang, P. Zhu, X. Ye, R. Liu and W. Cai, Precisely controllable oxygen vacancy-manufactured Ov-Co_3O_4@ PPy for high energy density supercapacitor, *Appl. Surf. Sci.*, 2022, **606**, 154863.
161 L. Wang, X. Xie, K. N. Dinh, Q. Yan and J. Ma, Synthesis, characterizations, and utilization of oxygen-deficient metal oxides for lithium/sodium-ion batteries and supercapacitors, *Coord. Chem. Rev.*, 2019, **397**, 138–167.
162 J. Militký, D. Křemenáková, M. Venkataraman and J. Večerník, Exceptional electromagnetic shielding properties of lightweight and porous multifunctional layers, *ACS Appl. Electron. Mater.*, 2020, **2**(4), 1138–1144.
163 J. Hao, S. Peng, H. Li, S. Dang, T. Qin, Y. Wen, J. Huang, F. Ma, D. Gao and F. Li, A low crystallinity oxygen-vacancy-rich Co_3O_4 cathode for high-performance flexible asymmetric supercapacitors, *J. Mater. Chem. A*, 2018, **6**(33), 16094–16100.
164 J. Wang, Z. Wang, B. Huang, Y. Ma, Y. Liu, X. Qin, X. Zhang and Y. Dai, Oxygen vacancy induced band-gap narrowing and enhanced visible light photocatalytic activity of ZnO, *ACS Appl. Mater. Interfaces*, 2012, **4**(8), 4024–4030.
165 S.-J. Park, J.-P. Lee, J. S. Jang, H. Rhu, H. Yu, B. Y. You, C. S. Kim, K. J. Kim, Y. J. Cho and S. Baik, *In situ* control of oxygen vacancies in TiO_2 by atomic layer deposition for resistive switching devices, *Nanotechnology*, 2013, **24**(29), 295202.
166 S. Yang, Y. Liu, Y. Hao, X. Yang, W. A. Goddard III, X. L. Zhang and B. Cao, Oxygen-vacancy abundant ultrafine Co_3O_4/graphene composites for high-rate supercapacitor electrodes, *Adv. Sci.*, 2018, **5**(4), 1700659.
167 K. Xiang, Z. Xu, T. Qu, Z. Tian, Y. Zhang, Y. Wang, M. Xie, X. Guo, W. Ding and X. Guo, Two dimensional oxygen-vacancy-rich Co_3O_4 nanosheets with excellent supercapacitor performances, *Chem. Commun.*, 2017, **53**(92), 12410–12413.
168 Y. Zhang, Y. Hu, Z. Wang, T. Lin, X. Zhu, B. Luo, H. Hu, W. Xing, Z. Yan and L. Wang, Lithiation-induced vacancy engineering of Co_3O_4 with improved faradaic reactivity for high-performance supercapacitor, *Adv. Funct. Mater.*, 2020, **30**(39), 2004172.
169 P. Cui, Y. Zhang, Z. Cao, Y. Liu, Z. Sun, S. Cheng, Y. Wu, J. Fu and E. Xie, Plasma-assisted lattice oxygen vacancies engineering recipe for high-performing supercapacitors in a model of birnessite-MnO_2, *Chem. Eng. J.*, 2021, **412**, 128676.
170 T. Zhai, S. Xie, M. Yu, P. Fang, C. Liang, X. Lu and Y. Tong, Oxygen vacancies enhancing capacitive properties of MnO_2 nanorods for wearable asymmetric supercapacitors, *Nano Energy*, 2014, **8**, 255–263.
171 Z. Xue, L. Lv, Y. Tian, S. Tan, Q. Ma, K. Tao and L. Han, Co_3S_4 nanoplate arrays decorated with oxygen-deficient CeO_2 nanoparticles for supercapacitor applications, *ACS Appl. Nano Mater.*, 2021, **4**(3), 3033–3043.
172 J. Zhang, H. He, X. Wang, G. Mao, W. Yu, Z. Ding, Q. Tian, H. Tong and X. Guo, A new modification strategy for improving the electrochemical performance of high-nickel cathode material: V_2O_5 particles anchored on rGO sheets as a dual coating layer, *Appl. Surf. Sci.*, 2022, **589**, 152878.
173 J. Zhao, Z. Li, T. Shen, X. Yuan, G. Qiu, Q. Jiang, Y. Lin, G. Song, A. Meng and Q. Li, Oxygen-vacancy Bi_2O_3 nanosheet arrays with excellent rate capability and $CoNi_2S_4$ nanoparticles immobilized on N-doped graphene nanotubes as robust electrode materials for high-energy asymmetric supercapacitors, *J. Mater. Chem. A*, 2019, **7**(13), 7918–7931.
174 J. Yang, X. Xiao, P. Chen, K. Zhu, K. Cheng, K. Ye, G. Wang, D. Cao and J. Yan, Creating oxygen-vacancies in MoO_{3-x} nanobelts toward high volumetric energy-density asymmetric supercapacitors with long lifespan, *Nano Energy*, 2019, **58**, 455–465.
175 X. D. Liu, Q. Yang, L. Yuan, D. Qi, X. Wei, X. Zhou, S. Chen, L. Cao, Y. Zeng and J. Jia, Oxygen vacancy-rich WO_3 heterophase structure: A trade-off between surface-limited pseudocapacitance and intercalation-limited behaviour, *Chem. Eng. J.*, 2021, **425**, 131431.
176 M. Kang, S. Zhou, J. Zhang, F. Ning, C. Ma and Z. Qiu, Facile fabrication of oxygen vacancy-rich α-Fe_2O_3 microspheres on carbon cloth as negative electrode for supercapacitors, *Electrochim. Acta*, 2020, **338**, 135820.
177 F. Han, J. Xu, J. Zhou, J. Tang and W. Tang, Oxygen vacancy-engineered Fe_2O_3 nanoarrays as free-standing electrodes for flexible asymmetric supercapacitors, *Nanoscale*, 2019, **11**(26), 12477–12483.
178 Z. Cao, C. Liu, Y. Huang, Y. Gao, Y. Wang, Z. Li, Y. Yan and M. Zhang, Oxygen-vacancy-rich $NiCo_2O_4$ nanoneedles electrode with poor crystallinity for high energy density all-solid-state symmetric supercapacitors, *J. Power Sources*, 2020, **449**, 227571.
179 D. Yan, W. Wang, X. Luo, C. Chen, Y. Zeng and Z. Zhu, $NiCo_2O_4$ with oxygen vacancies as better performance electrode material for supercapacitor, *Chem. Eng. J.*, 2018, **334**, 864–872.
180 H. Du, J. Lei, K. Xiang, W. Lin, J. Zheng and H. Liao, Facile synthesis of $NiCo_2O_4$ nanosheets with oxygen vacancies for aqueous zinc-ion supercapacitors, *J. Alloys Compd.*, 2022, **896**, 162925.
181 J. Wei, J. Guo, S. Wang, N. Ding, P. Xu, P. Wang, D. Han, Y. Wei and X. Yin, Fabrication of dual-functional electrodes using oxygen vacancy abundant $NiCo_2O_4$ nanosheets for advanced hybrid supercapacitors and Zn-ion batteries, *Inorg. Chem. Front.*, 2022, **9**(17), 4452–4463.
182 Y. Feng, W. Liu, Y. Wang, W. Gao, J. Li, K. Liu, X. Wang and J. Jiang, Oxygen vacancies enhance supercapacitive performance of $CuCo_2O_4$ in high-energy-density asymmetric supercapacitors, *J. Power Sources*, 2020, **458**, 228005.
183 S. Liu, Y. Yin, D. Ni, K. San Hui, M. Ma, S. Park, K. N. Hui, C.-Y. Ouyang and S. C. Jun, New insight into the effect of fluorine doping and oxygen vacancies on electrochemical performance of Co_2MnO_4 for flexible quasi-solid-state asymmetric supercapacitors, *Energy Storage Mater.*, 2019, **22**, 384–396.
184 K. Xiang, D. Wu, Y. Fan, W. You, D. Zhang, J.-L. Luo and X.-Z. Fu, Enhancing bifunctional electrodes of oxygen vacancy abundant $ZnCo_2O_4$ nanosheets for supercapacitor and oxygen evolution, *Chem. Eng. J.*, 2021, **425**, 130583.
185 C. Huang, A. Gao, F. Yi, Y. Wang, D. Shu, Y. Liang, Z. Zhu, J. Ling and J. Hao, Metal organic framework derived hollow NiS@C with S-vacancies to boost high-performance supercapacitors, *Chem. Eng. J.*, 2021, **419**, 129643.
186 A. Tugirumubano, S. J. Vijay, S. H. Go, L. K. Kwac and H. G. Kim, Characterization of electromagnetic interference shielding composed of carbon fibers reinforced plastics and metal wire mesh based composites, *J. Mater. Res. Technol.*, 2019, **8**(1), 167–172.
187 H. Wang, X. Xu and A. Neville, Facile synthesis of vacancy-induced 2H-MoS_2 nanosheets and defect investigation for supercapacitor application, *RSC Adv.*, 2021, **11**(42), 26273–26283.
188 X. Han, J. Ge, J. Luo, Y. Wang, X. Zhao, F. Zhang and X. Lei, Construction of vacancies-enriched CuS/Fe_2O_3 with nano-heterojunctions as negative electrode for flexible solid-state supercapacitor, *J. Alloys Compd.*, 2022, **916**, 165443.
189 J. Zhang, Y. Li, X. Liang, Q. Liu, Q. Chen and M. Chen, Sulfur vacancies-engineered Ni_3S_{4-x} hollow microspheres with optimized anionic adsorption energy for high-performance supercapacitor, *Small*, 2022, **18**(7), 2106074.
190 Y. Tao, J. Yuan, X. Qian, Q. Meng, J. Zhu, G. He and H. Chen, Spinel-type $FeNi_2S_4$ with rich sulfur vacancies grown on reduced graphene oxide toward enhanced supercapacitive performance, *Inorg. Chem. Front.*, 2021, **8**(9), 2271–2279.
191 X. Zhu and S. Liu, Al_2O_3-assisted synthesis of hollow $CuCo_2S_4$ nanospheres with rich sulfur vacancies for hybrid supercapacitor, *Electrochim. Acta*, 2022, **427**, 140881.
192 B. Wang, A. J. Fielding and R. A. W. Dryfe, *In situ* electrochemical electron paramagnetic resonance spectroscopy as a tool to probe electrical double layer capacitance, *Chem. Commun.*, 2018, **54**(31), 3827–3830.

193 L. Kang, M. Zhang, J. Zhang, S. Liu, N. Zhang, W. Yao, Y. Ye, C. Luo, Z. Gong and C. Wang, Dual-defect surface engineering of bimetallic sulfide nanotubes towards flexible asymmetric solid-state supercapacitors, *J. Mater. Chem. A*, 2020, **8**(45), 24053–24064.
194 F. Lu, M. Zhou, W. Li, Q. Weng, C. Li, Y. Xue, X. Jiang, X. Zeng, Y. Bando and D. Golberg, Engineering sulfur vacancies and impurities in $NiCo_2S_4$ nanostructures toward optimal supercapacitive performance, *Nano Energy*, 2016, **26**, 313–323.
195 J. Luo, X. Zhou, Y. Dong, N. Jiang, Q. Zheng and D. Lin, Sulfur-deficient flower-like zinc cobalt sulfide microspheres as an advanced electrode material for high-performance supercapacitors, *J. Colloid Interface Sci.*, 2022, **628**, 631–641.
196 X. Qian, Y. Yin, Y. Lu, J. Xia, B. Huang, J. Sun, G. He and H. Chen, Construction of sulfur vacancies enriched hollow zinc cobalt bimetallic sulfides for high-performance supercapacitors, *J. Alloys Compd.*, 2022, **913**, 165191.
197 J. Zhao, H. Cheng, Z. Zhang, Y. Liu, J. Song, T. Liu, Y. He, A. Meng, C. Sun and M. Hu, The semicoherent interface and vacancy engineering for constructing Ni (Co) Se_2@ Co (Ni) Se_2 heterojunction as ultrahigh-rate battery-type supercapacitor cathode, *Adv. Funct. Mater.*, 2022, **32**(33), 2202063.
198 A. Chang, C. Zhang, Y. Yu, Y. Yu and B. Zhang, Plasma-assisted synthesis of $NiSe_2$ ultrathin porous nanosheets with selenium vacancies for supercapacitor, *ACS Appl. Mater. Interfaces*, 2018, **10**(49), 41861–41865.
199 S. Siddique, C. C. Gowda, R. Tromer, S. Demiss, A. R. S. Gautam, O. E. Femi, P. Kumbhakar, D. S. Galvao, A. Chandra and C. S. Tiwary, Scalable synthesis of atomically thin gallium telluride nanosheets for supercapacitor applications, *ACS Appl. Nano Mater.*, 2021, **4**(5), 4829–4838.
200 L. Xiao, F. Ji, J. Zhang, X. Chen and Y. Fang, Doping regulation in polyanionic compounds for advanced sodium-ion batteries, *Small*, 2023, **19**(1), 2205732.
201 B. Huang, W. Zhang, J. Chen, Y. Cui, C. Zhu and S. Yan, Research progress and prospects of Li-air battery in wearable devices, *J. Electrochem. Soc.*, 2023, **170**, 020506.
202 Q. Zhou, Y. Wu, J. Gautam, D. Wang, X. Jiang, Z. Ma, H. Zhang, L. Ni and G. Diao, The current state of electrolytes and cathode materials development in the quest for aluminum-sulfur batteries, *Coord. Chem. Rev.*, 2023, **474**, 214856.
203 C. Hou, Y. Hou, Y. Fan, Y. Zhai, Y. Wang, Z. Sun, R. Fan, F. Dang and J. Wang, Oxygen vacancy derived local build-in electric field in mesoporous hollow Co_3O_4 microspheres promotes high-performance Li-ion batteries, *J. Mater. Chem. A*, 2018, **6**(16), 6967–6976.
204 S. Lee, W. Jin, S. H. Kim, S. H. Joo, G. Nam, P. Oh, Y. K. Kim, S. K. Kwak and J. Cho, Oxygen vacancy diffusion and condensation in lithium-ion battery cathode materials, *Angew. Chem., Int. Ed.*, 2019, **58**(31), 10478–10485.
205 G. Cui, Y. Zeng, J. Wu, Y. Guo, X. Gu and X. W. Lou, Synthesis of nitrogen-doped KMn_8O_{16} with oxygen vacancy for stable zinc-ion batteries, *Adv. Sci.*, 2022, **9**(10), 2106067.
206 Y. Zhou, C. Wang, F. Chen, T. Wang, Y. Ni, N. Yu and B. Geng, Scalable fabrication of $NiCoMnO_4$ yolk-shell microspheres with gradient oxygen vacancies for high-performance aqueous zinc ion batteries, *J. Colloid Interface Sci.*, 2022, **626**, 314–323.
207 Y. Go, K. Min, H. An, K. Kim, S. E. Shim and S.-H. Baeck, Oxygen-vacancy-rich $CoFe/CoFe_2O_4$ embedded in N-doped hollow carbon spheres as a highly efficient bifunctional electrocatalyst for Zn–air batteries, *Chem. Eng. J.*, 2022, **448**, 137665.
208 M. Yuan, Z. Sun, Z. Wu, D. Wang, H. Yang, C. Nan, H. Li, W. Zhang and G. Sun, Tuning the oxygen vacancy of mixed multiple oxidation states nanowires for improving Li-air battery performance, *J. Colloid Interface Sci.*, 2022, **608**, 1384–1392.
209 F. Li, M. L. Li, H. F. Wang, X. X. Wang, L. J. Zheng, D. H. Guan, L. M. Chang, J. J. Xu and Y. Wang, Oxygen vacancy-mediated growth of amorphous discharge products toward an ultrawide band light-assisted $Li–O_2$ batteries, *Adv. Mater.*, 2022, **34**(10), 2107826.
210 H. Lin, L. Yang, X. Jiang, G. Li, T. Zhang, Q. Yao, G. W. Zheng and J. Y. Lee, Electrocatalysis of polysulfide conversion by sulfur-deficient MoS_2 nanoflakes for lithium–sulfur batteries, *Energy Environ. Sci.*, 2017, **10**(6), 1476–1486.
211 H. Song, T. Li, T. He, Z. Wang, D. Fang, Y. Wang, X. L. Li, D. Zhang, J. Hu and S. Huang, Cooperative catalytic Mo-S-Co heterojunctions with sulfur vacancies for kinetically boosted lithium-sulfur battery, *Chem. Eng. J.*, 2022, **450**, 138115.
212 R. Xu, H. Tang, Y. Zhou, F. Wang, H. Wang, M. Shao, C. Li and Z. Wei, Enhanced catalysis of radical-to-polysulfide interconversion *via* increased sulfur vacancies in lithium–sulfur batteries, *Chem. Sci.*, 2022, **13**(21), 6224–6232.
213 D. He, J. Liu, M. Wang, C. Liu, Y. Huo and Z. Rao, Enhancing adsorption and catalytic activity of marigold-like In_2S_3 in lithium-sulfur batteries by vacancy modification, *Chem. Eng. J.*, 2022, **427**, 131711.
214 Q. Lei, J. Zhang, Z. Liang, Y. Yue, Z. Ren, Y. Sun, Z. Yao, J. Li, Y. Zhao and Y. Yin, Synergistic engineering of sulfur vacancies and heterointerfaces in copper sulfide anodes for aqueous Zn-ion batteries with fast diffusion kinetics and an ultralong lifespan, *Adv. Energy Mater.*, 2022, **12**(21), 2200547.
215 D. Li, L. Zhao, Q. Xia, J. Wang, X. Liu, H. Xu and S. Chou, Activating MoS_2 nanoflakes via sulfur defect engineering wrapped on CNTs for stable and efficient $Li–O_2$ batteries, *Adv. Funct. Mater.*, 2022, **32**(8), 2108153.
216 Y. Tian, G. Li, Y. Zhang, D. Luo, X. Wang, Y. Zhao, H. Liu, P. Ji, X. Du and J. Li, Low-bandgap Se-deficient antimony selenide as a multifunctional polysulfide barrier toward high-performance lithium–sulfur batteries, *Adv. Mater.*, 2020, **32**(4), 1904876.
217 W. Yao, C. Tian, C. Yang, J. Xu, Y. Meng, I. Manke, N. Chen, Z. Wu, L. Zhan and Y. Wang, P-doped $NiTe_2$ with Te-vacancies in lithium–sulfur batteries prevents shuttling and promotes polysulfide conversion, *Adv. Mater.*, 2022, **34**(11), 2106370.
218 X. Y. Wang, S. Y. Liao, Y. J. Wan, H. P. Huang, X. M. Li, Y. G. Hu, P. L. Zhu, R. Sun and C. P. Wong, Near-field and far-field EMI shielding response of lightweight and flexible MXene-decorated polyester textiles, *Mater. Today Phys.*, 2022, **23**, 100644.